3. MATERIALS PROCESSING TECHNOLOGIES

A. Laser Glazing and Friction Stir Processing of Materials to Reduce Friction

Principal Investigator: George Fenske
Argonne National Laboratory
9700 S. Cass Avenue
Argonne, Illinois 60439
630-252-5190; fax: 630-252-4798; gfenske@anl.gov

Chief Scientist: James J. Eberhardt
(202) 586-9837; fax: (202) 587-2476; e-mail: James.Eberhardt@ee.doe.gov
Field Technical Manager: Philip S. Sklad
(865) 574-5069; fax:(865) 576-4963; e-mail:skladps@ornl.gov

Participants
Layo Ajayi, Argonne National Laboratory
Ron DiMelfi, Materials Research Development
Stan David, Oak Ridge National Laboratory

Contractor: Argonne National Laboratory
Contract No.: W-31-109-ENG-38

Objective

- Determine the potential of laser glazing to lower parasitic energy losses between the flange and rail in rail transport.
- Develop a fundamental understanding of the metallurgy associated with the formation of low-friction. surface layers during laser glazing processing, and how these layers reduce friction between rail and wheel.
- Determine the potential of laser glazing to improve fuel efficiency and component durability/reliability of critical engine/powertrain components.
- Evaluate the impact of friction stir processing techniques on the friction and wear of steel.

Approach

- Develop advanced laser glazing processes to form glazed regions on carbon steels.
- Perform benchtop tests, full-scale rig tests, and field tests of glazed steels and rails to quantify the impact of glazing and friction stir processing on parasitic friction losses.
- Characterize glazed and non-glazed steels to elucidate the impact of glazing and friction stir processing on the microstructure of steel (1080 steel).

Accomplishments

- Optimized laser processing conditions under which uniform glazed surfaces form on carbon steels
- Evaluated friction and wear performance of glazed (and unglazed) rail steel by using benchtop and wheel/rail rig tests.
- Evaluated friction and wear performance of friction stir processed steel using benchtop rig tests.
- Characterized the microstructure and hardness of glazed and friction stir processed steels.
- Developed a deformation theory for nanocrystalline materials to model friction in glazed steel.
- Demonstrated efficacy of laser glazing to reduce friction on a full-scale test rig using prototype wheels, loads, and speeds.
- Glazed a 40 foot long section of rail steel for high-tonnage rail tests.
- Evaluated the friction and wear performance of friction stir processed steel using benchtop test rigs.

Future Direction

- Perform high-tonnage field tests at the Association of American Railroads/Transportation Technology Center, Inc., Facility for Accelerated Service Testing (AAR/TTCI FAST) in Pueblo, Colorado.
- Characterize the microstructure of glazed rail subjected to AAR/TTCI FAST tests.
- Make go/no-go decision to proceed with development of rail glazing technology.
- If go/no-go decision is to proceed, establish project with a railroad track maintenance equipment and service organization.
- Identify critical engine and powertrain components that if treated by advanced laser-based processes would lower parasitic energy losses.

Introduction

Wheel/Rail interactions account for a significant fraction of the energy consumed in rail transport. Past studies have indicated that energy savings could be as high as 24% when friction at the wheel/rail interface is properly managed. The key aspect is control of the friction forces. At the locomotive, high friction between the rail (specifically the top of the rail) and the wheel is desired to ensure adequate traction to keep wheels from slipping and sliding when power is applied. Friction is also required under braking conditions to control the speed of downhill-bound trains or to bring a train to a safe stop. The trailing cars, however, require much lower friction levels under normal train operations. For these cars, a low, controllable friction is desirable and can significantly reduce the energy required to pull a train. Two regions account for most of the frictional losses between the wheel and the rail: the region between the top of the rail and the wheel tread, and the region between the wheel flange and the gage face of the rail. Current wheel/rail lubrication (e.g., application of degradable greases and lubricants) is inconsistently applied and often disengaged by train crews. The research described herein focuses on the development of a laser glazing technique that imparts a durable, low-friction surface to the gage face of the rails to reduce parasitic frictional losses between the flange and rail gage.

Recent changes within the portfolio of activities supported by DOE's Office of FreedomCAR and Vehicle Technologies have re-focused this project on applications to reduce parasitic energy losses in engine and powertrain components. Approximately 10 % of the energy consumed in an engine can be attributed to asperity and viscous friction. Furthermore, advanced concepts (low-sulfur fuels, exhaust gas recirculation (EGR), and aftertreatment devices) under consideration to reduce emissions will have significant impacts on the tribological system. Concerns over low-lubricity fuels, higher soot and acid loading of engine lubes, and lower levels of sulfur and phosphorous containing additives have been raised regarding their impact on component durability and reliability. Efforts are currently under way to evaluate the potential of

laser-based technologies to improve the durability and reliability of critical engine components operating under more demanding tribological environments imposed by the advent of new fuels and lubricant formulations. Efforts are also in progress to evaluate the tribological potential of friction-stir processing (FSP). Traditionally FSP was developed to join components – e.g., friction stir joining of aluminum. However, FSP may also have potential to modify surfaces – e.g., harden near surface regions, or introduce alloying elements into near surface regions. To this end, preliminary studies were initiated to evaluate the impact of FSP on the tribological properties of steel.

Approach

The objective of this activity was to develop an advanced laser modification process to form a glaze on the gage face of the rail. Initial results and models predicted the formation of a nanocrystalline surface layer that would impart low-friction properties at the interface. The tasks associated with this project involve:

- Process development (laser glazing)
- Microstructural characterization of laser-modified surfaces
- Development of a model (of surface deformation)
- Lab-scale friction and wear testing of laser-modified surfaces (glazed and shot-peened)
- Full-scale friction testing of laser glazed steel
- Glazing of full-scale rail segments for field tests, and
- For, friction-stir-processing, lab-scale friction and wear testing under dry and lubricated conditions.

Results

The development [1,2] of the laser glazing processes used in these studies was documented in the FY03 Annual Report. Several approaches were investigated: two involved laser glazing, while a third approach investigated a laser shock-peening technique. Parametric studies were performed to optimize the conditions under which a glazed layer forms on 1080 steel. For this purpose, an Electrox 1.6-kW pulsed neodymium doped yttrium aluminium garnet (ND:YAG) laser with fiber-optic beam delivery and special beam shaping optics was used in Argonne National Laboratory's (ANL's) Laser Applications Laboratory. Two approaches were developed: one involved a single pass of the laser over a given area, and the other involved multiple overlapping passes. The Knoop hardness of the martensitic glazed regions was 2-3 times greater than that of the substrate, depending on whether a single-pass (factor of 3 times harder) or multipass (slightly over 2 times harder) process was employed. A commercial laser glazing process that utilized high-power diode laser technology was also investigated. In this case, bars of 1080 steel were processed by a commercial vendor (NuVonyx) and subsequently tested at ANL.

Friction and wear studies were performed using a number of lab-scale systems. Block-on-ring tests performed by Falex Corp. showed static friction coefficients of ≈0.35-0.45 for untreated 1080 steel that dropped to values ranging from 0.2 to 0.4 for differing glazing conditions. Large-scale (using a glazed segment of rail and a full-size wheel) "block-on-ring" tests performed at the AAR/TTCI Pueblo facility showed the static friction coefficient of the untreated 1080 rail varied from 0.2 to 0.5, depending on the applied load, whereas the friction coefficient of the glazed regions varied from 0.1 to 0.25. Dynamic friction coefficients for the glazed regions varied from 0.2 to 0.35, depending on load, compared to 0.2 to 0.55 for unglazed regions.

Benchtop pin-on-disc tests at ANL used flats of 1080 steel, glazed and unglazed, that rubbed against stationary balls or pins (52100 steel, 1080 steel, 440C steel, or alumina). The tests revealed that the composition of the pin/ball had a significant impact on the friction coefficient. The general trend was that the glazing reduced the friction coefficient by 3-35%, depending on the material. The greatest reduction was for the alumina ball sliding against the 1080 steel, suggesting that a strong chemical adhesion mechanism may be active with the metallic counterparts.

Twin roller tests were conducted at ANL with 1045 steel rail and wheel discs that were through-hardened (Rc 40) or glazed. The glazing effectively reduced the friction coefficient from roughly 0.4 for

the unglazed condition to 0.3 for the glazed rail rotating against an unglazed 1045 steel counterpart.

Results of tests performed in a twin-roller test rig at the Canadian National Research Center WBB (Wheel, Bearing, and Brake) facility in Ottawa, Ontario were reported in the FY 2004 Annual Report. More detailed results can be found in reference 2. The WBB Facility uses conventional and instrumented full-scale wheelsets loaded against large 63-in. diameter rims that simulate the track. The system is designed to operate at prototypical speeds and loads (30 mph and 33,000 lb in these tests). The instrumented wheelset allowed continuous monitoring of the lateral, longitudinal and vertical forces during the tests – a feature that was used to measure differences between glazed and non glazed regions.

The WBB tests were performed to confirm the friction reductions observed in the lab-scale tests and to evaluate the durability of the glazed regions prior to installing glazed rail segments in the FAST loop at the AAR/TTCI facilities. A 180^{o} segment of the lower WBB wheel was sent to NuVonyx where two, 10-12 mm wide tracks were glazed along the circumference of the rim – one track along the gage face, and the second track on the top of the rail approximately 5 mm from the gage point.

A series of runs was performed over a 5-day period to evaluate the efficacy of the glazing to reduce lateral and longitudinal forces (e.g., reduce friction), and to evaluate the durability of the glazing after moderate tonnage. The friction measurements were performed with an instrumented wheelset that permitted direct measurement of the forces using strain gauges applied to the rotating wheels. These provided a continuous measurement of the lateral, longitudinal, and vertical forces.

The WBB tests showed friction reductions ranging from 8 to 50% depending on the angle of attack. After 1 million gross tons (MGT) exposure, the friction reduction ranged from 4 to 45%. Based on

these encouraging results, efforts were initiated to treat a 40 foot long segment of track and to test it on the FAST loop facility in Pueblo, Colorado. The results presented below describe the effort to glaze the rail which was recently installed in the FAST loop.

Glazing of the 40 foot long segment of rail was performed by NuVonyx Inc. using protocols previously established for the WBB tests in Ottawa. Two segments of rail were provided by the TTCI: one segment, 4 foot in length, which was used to optimize glazing conditions to produce a glazing depth of 1-1/2 mm, and the second segment, 40 feet in length that was glazed and returned to TTCI for installation in the FAST loop facility. The 40-foot length had been cut in half and then rejoined (welded) to evaluate the impact of the glazing process on welded sections.

Results from the optimization studies on the 4 foot long segment indicated the optimum speed required using a 3800 watt beam was 0.5m/s. Two overlapping passes were used to produce a 1" wide glazed track along the gauge face of the rail. Figure 1 shows a dye-penetrant image of a portion of the 4 foot long rail that had been treated with overlapping tracks. The image shows no evidence of cracking that occurred (and subsequently resolved) in prior development efforts at NuVonyx for the Ottawa tests.

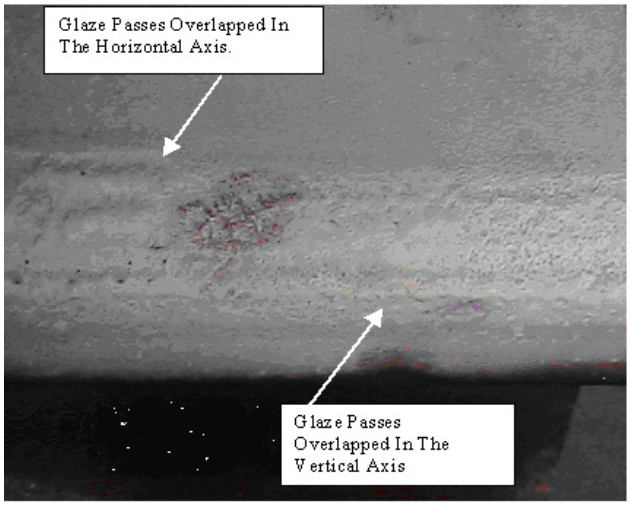

Figure 1. Dye-penetrant photograph of overlapped laser glazed tracks on 4-foot long trial rail.

With this assurance, effort proceeded to treat the 40 foot long segment. The entire 40 foot long segment was treated with two overlapping passes. Figure 2 shows a photograph of the rail during the glazing operation at NuVonyx. Post glazing dye-

penetrant analysis was performed on the 40-foot long segment. Figure 3 shows a section of the 40 foot long segment – in this case significant cracking was observed. The impact of the 'hockey-stick' cracks is not definitively known – these cracks were observed in optimization studies for the Ottawa tests, and great care was taken to optimize the spacing between the overlapping tracks to avoid the hockey-stick cracks. The Ottawa test optimization studies revealed the cracks occurred while the second overlapping track was applied and that it occurred in the overlap region on the first track. This is a concern that needs to be addressed in future development efforts and may involve the development of a single-pass glazing treatment.

The current status of the glazed rail project is that the glazed rail was returned to the TTCI where it was installed in the FAST loop for the next cycle of runs. Friction measurements will be made at periodic intervals during the FAST loop test period. After the runs are complete, sections of the glazed rail will be returned to ANL for microstructural characterization. Materials Research Development will prepare a proposal to the Transportation Research Board for follow-on research with NuVonyx, Harsco, and ANL to commercialize the process.

Investigation of the tribological properties of FSP'd steel was initiated in FY05 in collaboration with Oak Ridge National Laboratory (Dr. Stan David). Several plates of 1080 steel were prepared for FSP'ing at ORNL. Figure 4 shows a photograph of the plate in the as-treated condition. Two FSP'd tracks/regions were produced: one with a single pass treatment, and the second with multiple overlapping tracks.

Microstructural examination of the plate revealed the base material was fully pearlitic with a Knoop hardness of 300 to 350. The FSP'd regions were martensitic with Knoop hardnesses ranging from 700 to 750. The depth of the hardened region was 4 to 6 mm.

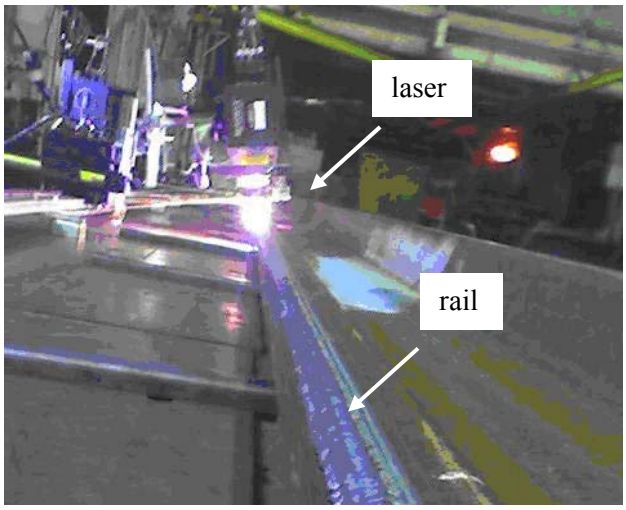

Figure 2. Photograph of the laser set-up used to glaze the 40 foot long rail.

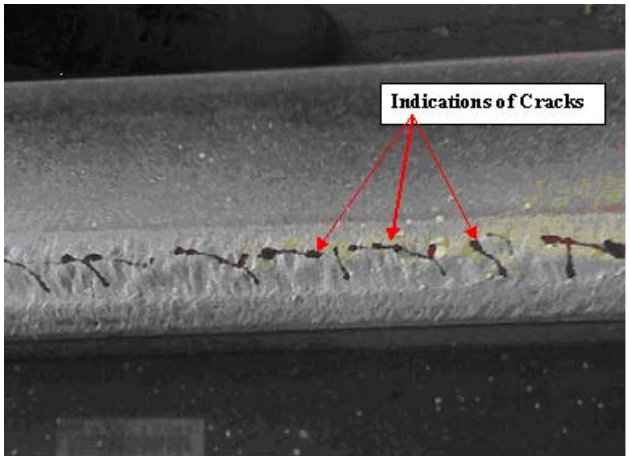

Figure 3. Dye-penetrant image of 40-foot long rail segment showing the presence of 'hockey-stick' cracks after overlapping tracks were applied.

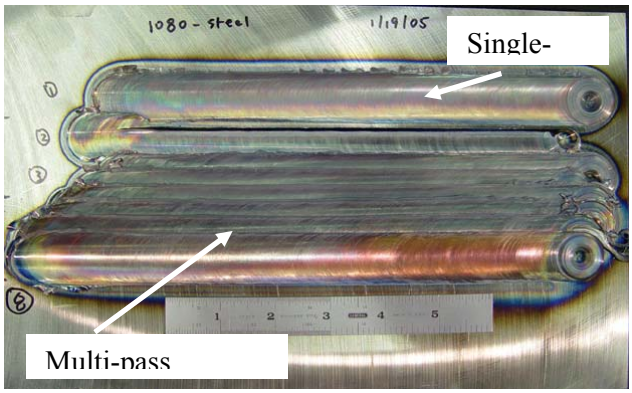

Figure 4. Photograph of a 1080 steel plate after single-pass and multi-pass friction stir processing.

Tribological tests were performed under dry and lubricated conditions using a pin-on-disc configuration on single and multi-pass test coupons. Prior to testing the rough surfaces were ground flat with a final grind using 320 grit SiC paper. The tribo tests were performed using a ½" diameter alumina ball sliding against the FSP'd coupons under a 10N load. The test duration was 1 hour at a sliding speed of 0.05 m/s. All tests were performed at room temperature in normal lab air (RH approximately 30 to 40 %). Tests were performed on single pass FSP steel, multi-pass FSP steel, and untreated steel under dry and lubricated (Mobil 1 10W-30 oil) conditions.

Results of the dry (open-air) and lubricated (Mobil 1 10W-30) tests are shown in figure 5 for the three different treatments. The untreated/reference coupon exhibited a friction coefficient of approximately 0.9, while the single or multi-pass surfaces exhibited friction coefficients of 0.7 – a significant reduction. Under lubricated conditions, all three surfaces appear to have similar friction coefficients close to 0.11, however, under closer examination (shown in the insert in figure 5, the multipass treatment appears to have a friction coefficient about 5 % lower than the single pass, or untreated surfaces.

The wear rates were also quantified after the tests. A 3-D optical microscope was used to measure the wear volume at multiple locations on the wear track. Under dry sliding conditions, the FSP'd coupons had wear rates approximately 1 order of magnitude lower than the untreated steel. Under lubricated conditions, no measurable wear was detected for the FSP's runs (1 hour in duration).

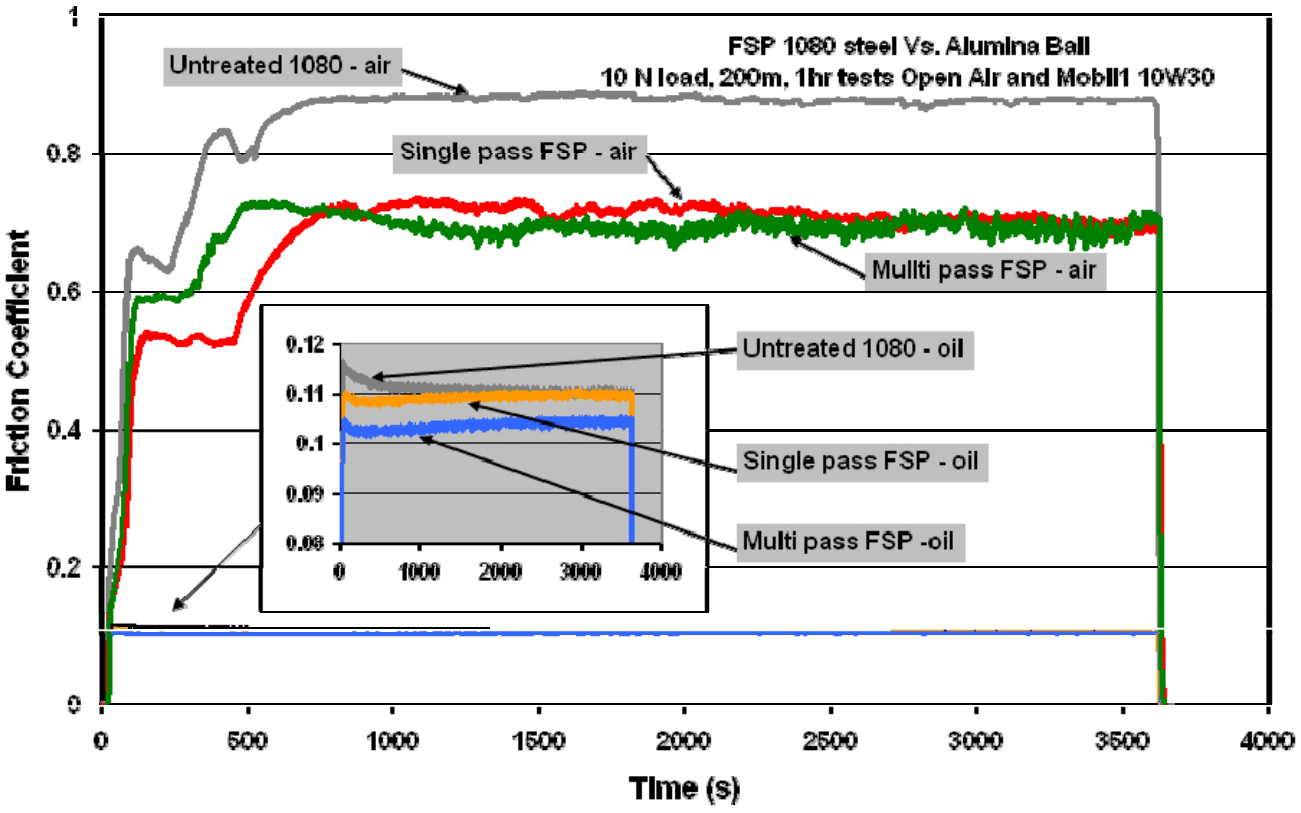

Figure 5. Graph of the friction coefficient of friction stir processed (and non-processed) 1080 steel as a function of time under dry and lubricated conditions.

Conclusions

Testing of laser glazing to improve the friction (and wear) performance of steels continues to progress. Initial lab-scale tests showed significant friction reductions and the more recent studies at Canadian National Research Council (CNRC), Ottawa have confirmed the friction reductions using full-scale wheels under high loads and prototypical speeds. Friction reductions in the range of 10 to 40 % have been observed – the magnitude of the reduction being dependent on the yaw and side loading. Efforts are in progress to establish a team to commercialize this technology with a rail maintenance firm. A 40-foot long track segment was glazed and installed in the FAST loop at the AAR/TTCI facility in Pueblo. The FAST loop tests are designed to put significant levels of tonnage on the treated track (upwards of 100 MGT). If successful, arrangements are being made to incorporate a laser-glazing system on a rail maintenance vehicle.

Efforts have also been initiated to explore the use of laser-glazing processing to treat engine and powertrain components. The increased hardness of near surface regions produced with laser-based processing may have significant impact on improving the durability of critical components (e.g., cylinder liners) that will be prone to accelerated wear with high levels of EGR.

Preliminary lab tests were performed on friction stir processed 1080 steel. The FSP produced a relatively thick, hard martensitic region that lowered friction under dry and lubricated conditions. Wear was lowered by at least one-order of magnitude.

References

1. S. H. Aldajah, O.O. Ajayi, G. R. Fenske, C. Reed, and Z. Xu, “Effect of Laser Surface Modifications on Tribological Performances of 1080 Carbon Steel”, submitted to ASME Journal of Tribology, October, 2004.
2. Laser Glazing of Rails WBB/IWS Tests (CNRC-Ottawa), Saud Aldajah, George Fenske, and Layo Ajayi (Energy Technology Division - ANL), Claude Reed and Zach Xu (Technology Development Division – ANL), and Ron DiMelfi (Materials Research Development), ANL Report ANL-05/03, January 2005.

B. Development of an Advanced Squeeze Casting (ASC) Process for the Production of High-Integrity Truck Components

Principal Investigator: David C. Weiss
Eck Industries, Incorporated
1602 North 8th Street, Manitowoc, WI 54221-0967
(920) 682-4618; fax: (920) 682-9298; e-mail: dweiss@eckindustries.com

Chief Scientist: James J. Eberhardt
(202) 586-9837; fax: (202) 587-2476; e-mail: James.Eberhardt@ee.doe.gov
Field Technical Manager: Philip S. Sklad
(865) 574-5069; fax:(865) 576-4963; e-mail:skladps@ornl.gov

Contractor: Eck Industries, Inc.
Contract No.: 4000022893

Objective

- Develop the equipment and process technology for an advanced squeeze casting (ASC) process to enable production of high-integrity cast metal components.
  - Integrate the advantages of two casting methods – low-pressure permanent mold and direct squeeze casting – to attain non-turbulent fill of the die, high solidification rates to refine microstructural features, and solidification under pressure to minimize microporosity.
  - Design and build a new kind of casting machine and develop process technologies needed to cast high-integrity truck components from nonferrous alloys.

Approach

- Design and construct a casting machine that integrates a low-pressure metal delivery system suitable for either aluminum or magnesium alloys, reliable gate shut-off technology, and direct application of squeeze pressures up to 103 MPa (15,000 psi). This machine is intended for production.
- Develop a gate shut-off mechanism that will operate reliably in a production environment.
- Select a casting that will be produced in the casting machine built for this project.
- Use fluid-flow and solidification analysis to predict optimum flow conditions for metal entering the mold and differential squeeze pressure requirements.
- Design and build cast tooling.
- Develop process technologies for the low-pressure/squeeze casting of aluminum alloys and evaluate the effect of various process parameters on casting integrity.
- Apply developed technologies to the production of a selected automotive component.

Accomplishments

- Fabrication of ASC machine has been completed and the machine installed at Eck Industries, Inc., Manitowoc, WI.
- Squeeze cast tooling designed and fabricated.

Future Direction

- Develop ASC process parameters for prototype production of B356-T6 connecting rods.

- Determine static and dynamic properties of ASC processed B356-T6.
- Demonstrate production viability of ASC casting machine and process.

Introduction

Squeeze casting is the solidification of liquid metal under pressure in a closed metal die. The resultant casting has improved properties and a more uniform microstructure as compared to those produced by traditional molten metal fabrication techniques. The higher properties are achieved through controlled entry of the metal into the die through large gates, which reduces turbulence, and high solidification rates with resultant refinement of microstructural features.

There are two squeeze casting methods--direct and indirect. The method and efficiency of pressure application distinguish the two processes. Direct squeeze casting applies pressure directly on the casting. This contrasts with indirect squeeze casting where pressure is applied via the gating system. The length of the gating system and any partial solidification prior to complete solidification of the part reduces the magnitude of the pressure applied and may result in casting porosity. For the indirect squeeze cast method the dimensions of the die cavity control part dimensions. For the direct squeeze cast method, the part dimensions are controlled by the die cavity dimensions and the finish position of the top die. Thus, the direct squeeze cast method requires precise machine control to attain the desired part dimensions. In addition, the direct method requires in-gate shut-off technology to control pressure during cavity pressurization. Both methods suffer from poor metal handling from the furnace into the mold or gating system. Inadequate control of pouring speed generates turbulence and casting defects such as oxide inclusions that reduce fatigue properties.

Earlier attempts to improve the squeeze casting process by combining the advantages of low-pressure die fill with those of squeeze casting demonstrated substantial mechanical property improvement and reduced component porosity. However, continuous production operation of the equipment was not achieved. The machines used were not specifically designed to meet the needs of the process.

Technical Approach

The results of this project will provide (1) a production viable ASC machine, (2) process technology that will improve the strength and reliability of cast automotive components, and (3) demonstrated production viability of the equipment and process.

Machine Design. Previous efforts had demonstrated that modification of current cast machine designs would not provide a production capable ASC machine. An assessment of the capabilities and limitations of current machine designs demonstrated that:

- Low-pressure cast equipment typically does not have the structural rigidity needed to withstand the high pressures required of squeeze casting.
- Die-casting and currently available squeeze casting machines are not designed for proper (non-turbulent) molten metal entry into the die cavity.
- Neither type of equipment is typically available with the hydraulic and electronic controls necessary to attain the die cavity motions required for the direct squeeze casting process.

After much consideration, the project team decided it was easier and more cost effective to build a machine from the “ground up” than to modify an existing cast machine design. To facilitate this design and construction, the team partnered with Empire Castings, Inc., an experienced producer of low-pressure casting equipment.

Process Development. Bendix, Inc. is an industrial manufacturer of truck components with an interest in reducing manufacturing cost by the use of high quality castings. Consultation with them led to the selection of an air compressor connecting rod for prototype production in the ASC machine. This component has a level of complexity that can demonstrate the production capability of the ASC machine and process, the need for mechanical properties higher than those attainable with

commercially available castings, and provides an opportunity for production with the ASC process.

The cast part was modeled for fluid flow and solidification. This work was done in parallel with equipment design. Simulation provided an understanding of optimum metal flow conditions and squeeze requirements, if any, to contend with solidification shrinkage. This is very important to the success of the program and, potentially, to the details of the machine design. The ASC machine has two mechanisms to feed the casting—low-pressure, nonturbulent fill of the die cavity and high-pressure, direct squeeze to minimize solidification shrinkage. Modeling experiments were used to explore the interaction of the two feed mechanisms and select process parameters that lead to process optimization. Modeling results were used to refine the die design and select initial casting process parameters.

After tooling construction and ASC machine delivery, castings will be made under the range of process conditions anticipated during modeling. A variety of both cast and wrought alloys (Table 1) will be used. Evaluation of those castings will include radiography, die penetrant inspection, tensile testing, and functional component testing at Bendix. It is anticipated that this part of the program will require multiple iterations to produce the desired product quality. Some equipment and tooling modification may be required during this part of the program.

Table 1. Aluminum alloys to be used for casting trials

AA 380	AA 206
AA 356	AA 6061
AA 357	AA 535
AA 319	AA 388

After successful production of development castings, the production viability of the equipment and process will be demonstrated. This will be done by:

- Production of a connecting rod with reduced porosity and improved mechanical properties as compared to the current die-cast connecting rod used by Bendix.
- Continuous production with the ASC machine and connecting rod tooling to include at least one 5-h continuous run with the equipment running at least three days in a week.

The goal of the project team is to implement part production on an ongoing basis. The production phase of the project will include detailed cost analysis of part production, determination of die-life parameters, and ongoing equipment and tooling development for maximum uptime.

Program Schedule

The revised scheduled start and end dates for the various program tasks are listed in Table 2.

Table 2. Overall program schedule (revised).

Program Task	Start Date	Finish Date
Machine design	June 2003	Feb. 2004
Machine build	Mar. 2004	Nov. 2004
Tooling design	July 2003	Oct. 2003
Tooling build	Nov. 2003	Mar. 2004
Process Model	Oct. 2004	Dec. 2004
In-gate S.O. development	Nov. 2003	Dec. 2003
Machine install	Nov. 2004	Nov. 2004
Casting development	Dec. 2004	Dec. 2005
Evaluation & Testing	Jan. 2006	Mar. 2006
Final Report	Jan. 2006	Mar. 2006

Program Status

ASC Machine. The design (Figure 1) for the 600-ton capacity ASC machine has been completed. Positioning of the top die is accomplished independently of the squeeze-cast cylinder. To

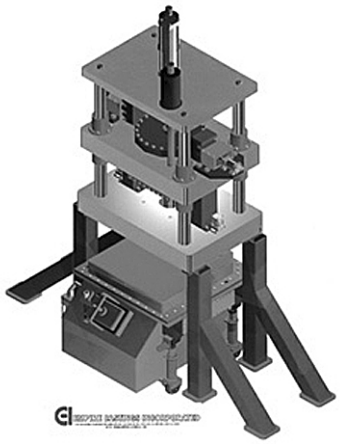

Figure 1. Design for 600-ton ASC machine.

maximize machine capability, the melting vessel is equipped with a crucible furnace. This facilitates the melting of both cast and wrought aluminum and magnesium alloys as well as aluminum and magnesium metal matrix composite alloys.

To match the dimensional capabilities of the die-cast process, a closely controlled volume of liquid metal must be fed into the die cavity. Conventional low-pressure fill technology does not have the capability to accurately meter a fixed amount of liquid metal into the die. Therefore, we will accurately position (± 0.13 mm) the top die to obtain the desired fill volume and use a fill sensor and an independently controlled gate shut-off to control metal volume. Development of a reliable gate shut-off technology is a key part of the experimental program. Gate shut-off system components are shown in Figure 2.

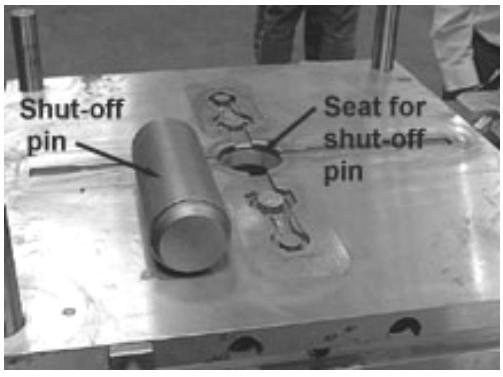

Figure 2. Components of in-gate shut-off system.

The machine (Figure 3) has been installed at Eck Industries, Inc., Manitowoc, WI.

Data Acquisition System. A computerized data acquisition system has been designed to interface with the displacement, pressure and temperature sensors located on the ASC press and cast tooling. Analysis of these data will be critical in understanding the operation of the ASC process. A plot of a typical data set is shown in Figure 4.

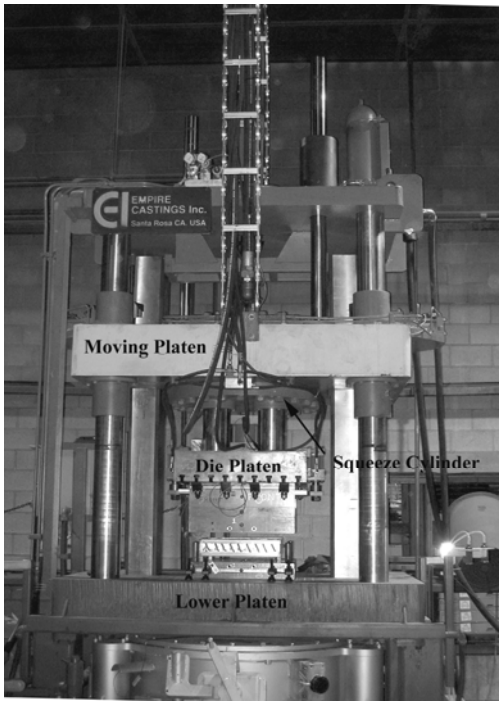

Figure 3. ASC Machine installed at Eck Industries, Manitowoc, WI

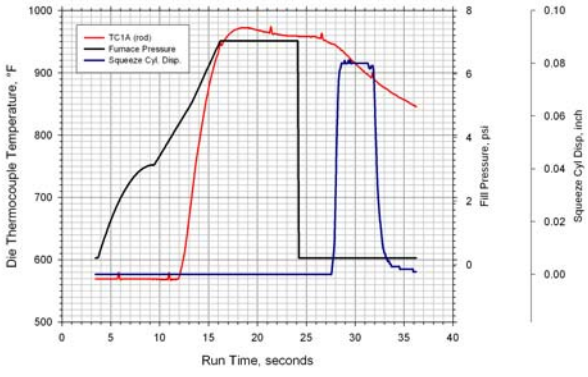

Figure 4. Typical data obtained from data collection system during casting runs.

Cast Tooling. The die for casting air-compressor connecting rods and tensile test bars has been completed. As shown in Figure 5, the tooling consists of a die holder and individual die inserts for the particular part being cast. This tooling will be used for process development and the machine run-off trials.

Process Development. Early development trials demonstrated that the use of temperature data from the thermocouples installed in the tooling does not provide consistent operation of the ASC machine. Therefore, the PLC program was modified to control sequencing of the machine operations by a combination of adjustable timers and thermocouple inputs from the tooling. Thermocouple inputs are used to initiate the sequence and determine when the die is opened after the squeeze pressure application has been completed. All other functions are controlled by timers.

This modification to the machine's PLC program was proven successful by the sequential accomplishment of 40 castings. A typical casting is shown in Figure 6. A few connecting rod castings have been machined to determine if the as-cast dimensions meet Bendix's requirements. Figure 7 shows a machined connecting rod and an as-cast part after the gating has been removed. The connecting rod castings meet the part dimensional requirements.

Preliminary tensile data (see Table 3) show the ASC processed alloy to have about the same properties permanent mold cast material of the same chemistry but the elongation values are significantly higher. The higher elongation value may be the result of either smaller grain size because of the higher solidification rates or lower porosity levels.

Figure 5. View of cast tooling.

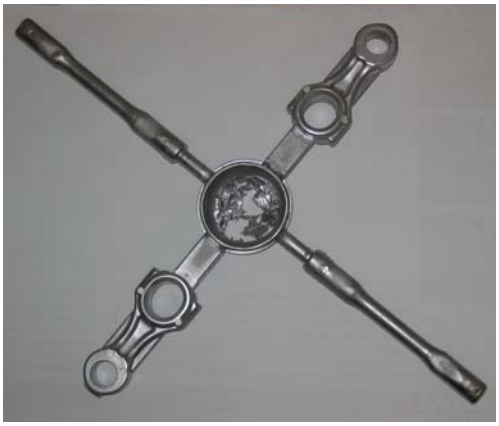

Figure 6. Typical casting from 40 shot run.

Figure 7. Machined (left) and as-cast (right) connecting rod parts.

Table 3. Preliminary mechanical property results.

B356-T6	LPPM Cast	ASC Cast
Ultimate Strength, ksi	39.0	41.8
Yield Strength, ksi	26.6	25.7
Percent Elongation	5.8	15.5

Conclusions

Good progress has been made on the project. Consistent operation of the ASC machine has been obtained. Casting trials are in progress to develop the specific parameters needed to produce test bars and connecting rods from which mechanical properties and performance data may be obtained. As shown in Table 2, the schedule has been revised to reflect expected completion dates.

C. Wrought Magnesium Alloy/Process Development

Principal Investigator: J. A. Horton
Oak Ridge National Laboratory
P.O. Box 2008, Oak Ridge, TN 37831-6115
(865) 574-5575; fax: (865) 574-7659; hortonja@ornl.gov

Principal Investigator: S. R. Agnew
University of Virginia
116 Engineer's Way
P.O. Box 400745, Charlottesville, VA 22904-4745
(434) 924-0605; e-mail: agnew@virginia.edu

Chief Scientist: James J. Eberhardt
(202) 586-9837; fax: (202) 586-1600; e-mail: james.eberhardt@ee.doe.gov
Field Technical Manager: Philip S. Sklad
(865) 574-5069; fax: (865) 576-4963; e-mail: skladps@ornl.gov

---

Contractor: Oak Ridge National Laboratory
Contract No.: DE-AC05-00OR22725

Objectives

- Develop wrought magnesium alloys with better formability than current magnesium alloys.
- Investigate new processing techniques for cost reduction and formability improvement.
- Contribute to basic understanding of deformation, processing, and alloy behavior for this lightweight metal.

Approach

Explore new processing schemes for magnesium alloy sheets; evaluate the practical formability of new alloys and after new processes; determine deformation mechanisms using experimentation and simulation.

Accomplishments

- Devised a new approach to substantially reduce texture development utilizing rare earth additions and a recrystallization step during hot rolling processing.
- Completed infrared rolling study on narrow strips of Mg sheet removed at various points during a commercial processor's rolling schedule.
- Found significant 0002 texture formation after hot rolling at temperatures from RT to 450°C.
- Demonstrated roll bonding as a technique to reduce grain size. Good metallurgical bonds were produced.
- Demonstrated feasibility of infrared processing of twin roll cast Mg sheet in collaboration with Norsk Hydro.
- Performed a study of the effect of grain size on deformation mechanism in alloy AZ31B. Found surprising result that mechanical twinning contributes significantly to tensile behavior of coarse-grain sheet.

Future Direction

- Interact with an industrial partner to advance commercialization of infrared processing for cost reductions.
- Define further correlations of microstructure, mechanisms, and anisotropy. In particular, define the kinetics and crystallography of recrystallization in magnesium alloys.
- Further explore superplastic-type behavior observed at warm forming temperatures.
- Investigate fundamental parameters affecting castability of the more creep-resistant alloys.

Introduction

Magnesium, with a density 66% of aluminum, has obvious advantages for use as a structural material in the transportation industry. Magnesium castings are steadily growing in use in autos and trucks. However, wrought applications are held back by the high cost of sheet due to the large number of processing steps. This project is currently focusing on processing techniques and issues to reduce the cost of sheet magnesium. In addition, we are continuing to investigate formability issues of sheet magnesium.

Infrared Processing Study of Magnesium Strip

Strips of magnesium sheet were extracted from midway thru the processing route from a commercial magnesium producer, Magnesium Elektron Corp (MEL). These strips were readily processed using infrared lamps and subsequent rolls in a lab table top setup. Grain size and properties were tracked. However, it was concluded that the widths used, ~50 mm, was insufficient to replicate commercial practice. A scale up to strips approximately 30 cm is planned.

0002 texture formation after hot rolling

Texture in hexagonal magnesium is unfortunately easily developed during thermomechanical processing thereby reducing fabricability. Many processing routes have been investigated to produce material with reduced texture. The following experiment was performed to find out if there was an optimum rolling temperature. AM60 was cast into a rectangular mold and then annealed 24 hr at 413°C. Three mm thick slabs were cut from this casting. This starting material had no 0002 texture. The slabs were then pack rolled one time sandwiched in stainless steel to retain the heat. The conditions were either 34% at 250°C, 42% at 350°C, or 54% at 450°C. Texture determinations were then performed, see Figure 1.

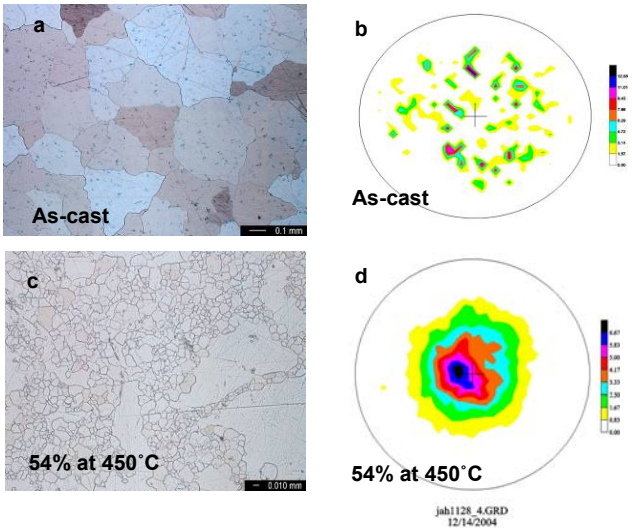

Figure 1. Optical micrographs and 0002 pole figures showing the degree of texture developed in just one pass at 450°C.

The intensity is approximately half of that of rolled commercial sheet after many trips through the rolling mill. The results from 250, 350 and 450°C were nearly identical. Just one pass through a rolling mill produces a substantial amount of 0002 texture. 450°C is a practical limit for such processing in air without running a risk of a runaway exothermic reaction.

Accumulative Roll Bonding

Commercial AZ31 sheets were roll bonded together (see Figure 2). This process results in severe plastic deformation which leads to a refinement of the microstructure and improvements in the mechanical properties. This technique is relatively simple and can be applied to large sheets. A maximum of 6 passes; resulting in a 64 layer bond was successfully achieved with approximately 60% reduction per pass. AZ31 was also roll clad with Al-alloy 6061 and good bonding was achieved.

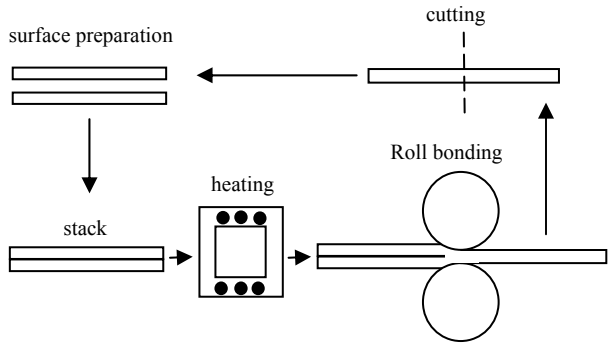

Figure 2. Schematic diagram of the accumulative roll bonding process

Roll bonding resulted in dynamic recrystallization (DRX) and a fine equiaxed grain size (down to 1 μm), see Figure 3. The bonding line is a very thin non-continuous oxide film in the Mg only bonds, in some areas grains appear to have grown across the bonding line. In tensile testing no delimitation of the bonds was observed. In the roll clad Mg-AL sample an intermetallic layer appears on the bonding line (Figure 3b); from EDS analysis it is likely that this is $Mg_{17}Al_{12}$. In tensile loading no delimitation resulting from the brittle intermetallic layer was observed.

The mechanical properties of the roll bonded/clad specimens are given in Table 1. The high temperature mechanical properties of the roll bonded specimens shows a remarkable improvement over the original material. Improvements in the roll bonding process shows potential to improve the mechanical properties and formability of magnesium alloys. Roll cladding of magnesium alloys should also be further investigated; this process may be used to improve the mechanical, physical and chemical properties of the alloys.

Twin Roll Cast Mg rolled to sheet using infrared heating

Direct twin roll cast Mg sheet with dimensions approximately 30 cm wide and 6 mm thick was obtained from Norsk Hydro. This material was further rolled down to 1 mm thickness using quick infrared lamp anneals and heating to 415°C between 20% reduction passes. Figure 4 shows the optical microstructure after the 7th pass and a 1 mm in thickness. Use of twin roll casting and infrared heating could together substantially reduce the cost of Mg alloy sheet.

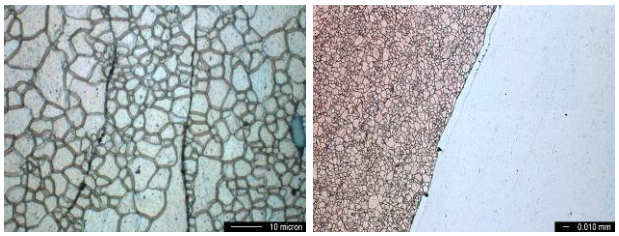

(a) (b)

Figure 3. Optical micrographs of (a) AZ31 64 layer roll bond. Three layers can be seen in the figure; the layer thickness is 20-50 μm. and (b) cross section of Al-Mg-Al roll clad sample, the etched microstructure is AZ31 and Al-alloy 6061 is unetched.

Table 1. Tensile properties of the roll bonded samples at room temperature (RT) and at 400°C tested parallel to the rolling direction at a strain rate of 1x10-3 s-1.

	RT		400°C	
	ε_f (%)	UTS (MPa)	ε_f (%)	UTS (MPa)
AZ31-H24 (original material)	12.2	294.5	37.9	20.5
AZ31-64 layers	9.0	234.0	137.9	22.6
Al-Mg-Al	15.2	199.5	64.8	29.5

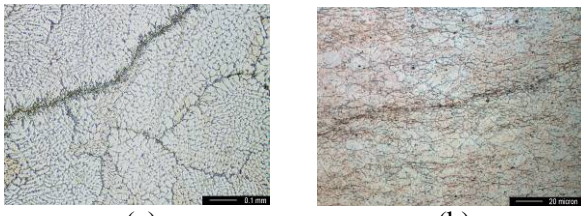

(a) (b)

Figure 4. Optical micrographs of twin roll cast as cast (a) and after rolling 7 times with infrared anneals (b) to 1 mm thickness.

Equal channel angular extrusion (ECAE)

At the University of Virginia, we have been completing our examination of equal channel angular extrusion of magnesium alloys to close two studies. One is a close examination of the texture evolution enforced by ECAE upon 5 different wrought magnesium alloys (AZ31, AZ80, ZK60, WE43, and Mg-4wt%Li.) The texture evolution of these alloys was modeled using a polycrystal plasticity code, enabling inferences regarding the deformation mechanism activity of the different alloys to be made. In terms of their texture evolutions, the alloys may be classified into three groups, the zirconium-, the aluminum-, and the

lithium-containing. Based upon the modeling, these appear to be connected with a preference for slip of <c+a>, balanced non-basal <a> and <c+a>, and non-basal <a> dislocations, respectively. It is also mentioned that the texture evolution of the WE alloy is particularly unique, in that it possesses a rather weak texture throughout its processing history. (This latter result was an important finding that went unnoticed until recently and corroborates other findings reported below.) These studies have resulted in two journal publications listed at the end of this report.

In addition to examining the structure of magnesium alloys subjected to ECAE, we have continued to examine the mechanical properties, as a follow-up to our previously published work on the ductility enhancement of alloy AZ31. We have elected to examine the ductility enhancement of a heat-treatable magnesium alloy, AZ80. Although the highest magnitude of the obtained ductility is less impressive in this alloy (~28% vs. ~40%), the magnitude of the improvement over conventional processing (~2.5 times) is similarly impressive. Again, there appears to be a strong connection between the ductility enhancement and an unusual texture which results from ECAE processing. Age-hardening of the ECAE processed material succeeds in improving its strength; however, the combined property set (strength and ductility) is not superior to that obtained by conventional processing methods. This study has been submitted for publication and is presently in revision.

Effect of Grain Size Deformation Mechanisms of Magnesium Alloy AZ31

Beginning with the relatively small grain size of recrystallized AZ31 sheet (~13 μm), samples were annealed at high temperatures (up to 525°C) for a range of times to produce grain sizes up to 220 μm. Not surprisingly, the increase in grain size led to a decrease in both strength and ductility. Figure 5 shows that the data obey traditional expectations for the grain size dependence of yield strength, albeit with the effect of anisotropy superimposed.

Our study focused on the effect of grain size on the strain anisotropy, since our earlier investigations of sheet anisotropy had shown a link between strain anisotropy and deformation mechanism activity.

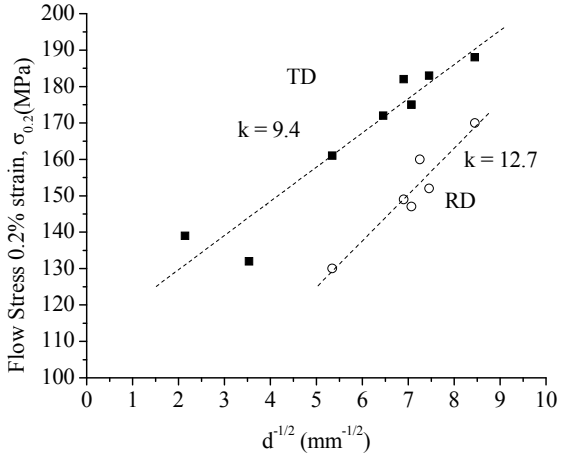

Figure 5. Hall-Petch plot of AZ31B strengths along the rolling (RD) and transverse directions (TD).

As a measure of anisotropy, we have relied on measurements of r-value, the ratio between Poisson strains along the sheet thickness direction and the sample width directions during a tensile test. Initially, it was found that the strain anisotropy after 11% tensile strain was virtually unaffected by grain size. We instituted the capability to measure the r-value evolution *in-situ*, and this provided a completely different picture (Figure 6). The instantaneous r-values increase with increasing grain size. Interestingly, {10.2} tensile twinning appears to be responsible, despite the fact that the texture and imposed stress direction would appear to preclude activation of this mechanism during these tensile tests.

The observations of this study, as well as those of a parallel study sponsored by the National Science Foundation, suggest that certain types of mechanical twinning are potential aides to ductility (note ECAE results above) while other types of twinning may serve as failure mechanisms. Control of the texture and grain size has been a consistent theme of our research program and the present results further emphasize the need to pursue this goal to control the influence of mechanical twinning mechanisms.

Neutron Diffraction Studies of Deformation Mechanisms of Magnesium

In-situ neutron diffraction techniques have been used to determine the internal stresses that develop within magnesium alloy AZ31 under load. Using an

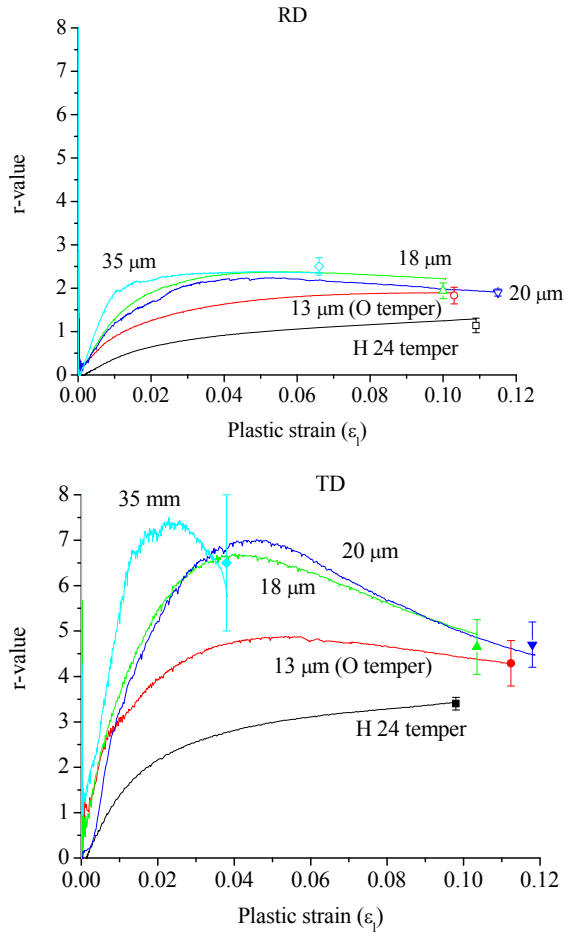

Figure 6. Measured r-value evolution with strain for samples tested along the (RD) rolling direction and (TD) transverse direction with different grain sizes.

inverse method involving an internal stress data have been used to assess the critical stresses and activities of the various deformation mechanisms with magnesium alloys. Specifically, we have used neutron diffraction to compare conventional and ECAE processed material. These experiments provided further evidence in support of the hypothesis which we published previously, that due to the unusual ECAE texture, the soft mechanisms (basal slip and mechanical twinning) are able to accommodate the imposed strain. Because this keeps the flow stress low, it helps to explain why the ductility is enhanced in this material which appears to fail at a critical stress level. Not only have these results been useful for developing a greater understanding of magnesium, the data have also served an important role of validating a modeling code (EPSC) which is of use for many materials.

Figure 7 shows results obtained from a larger grained sample of AZ31 sheet from the grain size study described above. The ex-situ (00.2) pole-figure data indicate that mechanical twinning has taken place (Figure 7a); however, it was initially unclear if the twinning happened during the deformation or during unloading. The in-situ measurement of the (00.2) diffraction peak intensity shows that the twinning was indeed happening during the deformation. As discussed above, this is a much unexpected result, given the crystallography of twinning and the stressing direction. However, they will provide a basis for determining why twinning is so pervasive in magnesium alloys under straining conditions where twinning is unexpected (i.e., during rolling of sheet, during tensile deformation of rolled sheets, extrusions, etc.).

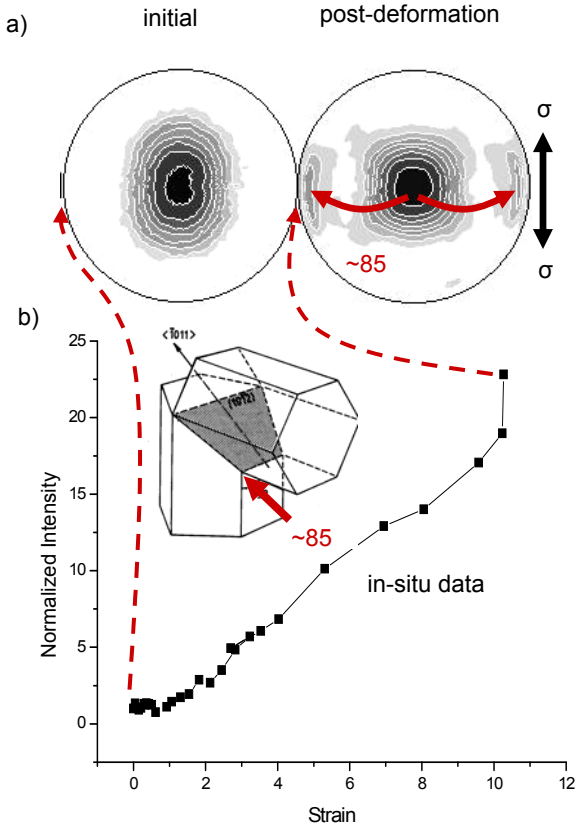

Figure 7. a) Initial and post-deformation basal (00.2) pole figures from tensile tests show evidence that twinning has occurred within grains of the dominant texture component. b) (00.2) diffraction peak intensities obtained using in-situ neutron diffraction show that the anomalous twinning occurs during the deformation, not after.

Wrought Alloy Development

Our work in past years has demonstrated that the mechanical behavior of magnesium alloys is strongly affected by crystallographic texture because of the intrinsic plastic anisotropy of the hexagonal close packed crystal structure. Indeed, conventional Mg alloy sheets exhibit strong textures (with basal planes parallel to the sheet plane) with little variation from one alloy to another. We have used this fact to our advantage to selectively study the mechanisms of plastic deformation, such as the study of twinning described above. However, it is certain to affect a positive change in the performance if the texture could be qualitatively altered. In fact, Dow Magnesium offered "special bending sheet" in years past, which was nothing more than a texture-altered alloy AZ31-O temper that had much better forming characteristics than conventional sheet (e.g., critical bending radius of 5 times the sheet thickness, versus 3 times.)

Until recently we had not devised a practical scheme to alter the strong textures that evolve during deformation processing. As described earlier in this report, we recently explored the effect of hot rolling at various temperatures and various recrystallization treatments at Oak Ridge National Laboratory (ORNL). Although there was some quantitative variation in the texture, the textures were all qualitatively the same, and did not promise to quantitatively alter the forming behavior.

It has been reported that alloy WE54 containing significant additions of expensive alloying additions, yttrium (W) and rare earth (E) elements, develop much weaker textures during extrusion than conventional alloys, and that the undesirable tension-compression strength asymmetry which plagues most magnesium extrusions was effectively eliminated [E.A. Ball and P. B. Prangnell, "Tensile-compressive yield asymmetries in high strength wrought magnesium alloys," Scripta Metall. Mater., 31 (1994) pp. 111-116, 1994]. The authors suggested that the result might be related to particle-stimulated nucleation of randomly oriented grains during recrystallization. More recent doctoral research of Luke Mackenzie at the University of Manchester on similar alloys provided more evidence that recrystallization phenomena were responsible for the texture randomization [G.W. Lorimer, L.W.F. Mackenzie, F.J. Humphreys, and T. Wilks, "The Recrystallization Behavior of AZ31 and WE43," Mater. Sci. Forum, 488-489 (2005) 99-102]. A new member of the project team, Jeremy Senn, has devised a plane strain compression fixture for enforcing rolling type deformation under controlled temperature and strain rate conditions. His recent results from WE53 confirm strong texture development during hot-rolling conditions and a very weak texture after recrystallization (Figure 8). These results suggest an avenue to improve the formability of Mg sheets by through careful alloying and thermomechanical treatment.

Finally, we have begun collaborating with researchers at the GKSS, Geestacht who provided us with a number of experimental alloys, which had been warm rolled in their facilities or by an industrial partner. These alloys are very different in composition from the ones mentioned above, yet have very weak textures, in comparison with conventional alloys, ZM21 containing Zn and Mn (or AZ31). Their mechanical behavior is very distinct from AZ31 on which we have focused in the past (some alloys are more ductile, and all exhibit much lower strain anisotropy.) Similarly, a press release from Primo Metal in Korea boasted the best warm forming behavior of any wrought magnesium alloy. They have sent us sheet samples and we have verified that this alloy has a very weak texture, and

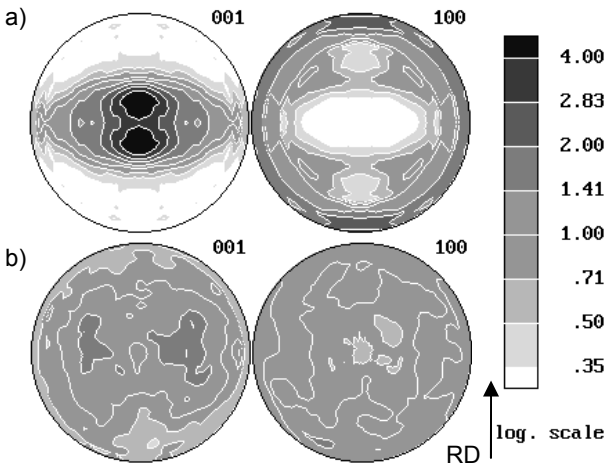

Figure 8. Textures measured in alloy WE53 produced at ORNL show a) strong texture after hot-rolling type deformation and b) very weak texture after recrystallization annealing of the same.

low strain anisotropy. Again, there does seem to be a path towards a sheet alloy with better forming characteristics.

Publications and Presentations

A. L. Bowles, Q. Han, J. A. Horton, "Castability of Magnesium Alloys" *Magnesium Technology 2005,* ed. by N. R. Neelameggham, H.I. Kaplan, and B.R. Powell, TMS (2005) 99-104.

J.A. Horton, C.A. Blue, T. Muth, A.L. Bowles, S.R. Agnew, "Infrared Processing of Magnesium Wrought Alloys" i*bid.,* 155-158.

S.R. Agnew and O. Duygulu, "Plastic Anisotropy and the Role of Non-basal Slip in Magnesium Alloy AZ31," *Inter. J. Plasticity*, 21 (2005) 1161-1193.

S.R. Agnew, D.W. Brown, and C.N. Tomé, "Validating a Polycrystal Model for the Elasto-Plastic Response of Magnesium Alloy AZ31 Using In-situ Neutron Diffraction," *submitted to Acta Mater.*

S.R. Agnew, P. Mehrotra, and T.M. Lillo, "Equal Channel Angular Extrusion of a Heat Treatable Magnesium Alloy," *Scripta Mater.*, *in revision*.

S.R. Agnew, P. Mehrotra, T.M. Lillo, G.M. Stoica, and P.K. Liaw, "Crystallographic Texture Evolution of Three Wrought Magnesium Alloys During Equal Channel Angular Extrusion," *Mat. Sci. Eng. A*, **408** (2005) 72-78.

S.R. Agnew, P. Mehrotra, T.M. Lillo, G.M. Stoica, and P.K. Liaw, "Texture Evolution of Five Wrought Magnesium Alloys During Route A Equal Channel Angular Extrusion: Experiments and Simulations" *Acta Mater.,* **53** (2005) 3135-3146.

D.W. Brown, S.R. Agnew, M.A.M. Bourke, T.M. Holden, S.C. Vogel and C.N. Tomé, "Internal Strain and Texture Evolution During Deformation Twinning in Magnesium," *Mat. Sci. Eng. A*., **399** (2005) 1-12.

D.W. Brown, S.R. Agnew, S. Abeln, W. Blumenthal, M.A.M. Burke, M. Mataya, C.N.Tome, and S.C.Vogel, "The role of texture, temperature and strain-rate in the activity of deformation twinning," *Mat. Sci. Eng. A,* **495-497**, (2005) 1037-1042.

Presentations w/o Publication

S.R. Agnew, O. Duygulu, and A. Jain, "Using Polycrystal Plasticity Simulation to Explore the Behavior of Wrought Magnesium Alloys," presented at "Plasticity 2005", Kauai, Jan. '05.

S.R. Agnew, O. Duygulu, and A. Jain, "Developing Mechanism-Based Models of the Mechanical Behavior of Wrought Magnesium Alloys" U. of Michigan, Dept. MSE Seminar Series, Ann Arbor, Feb. '05.

O. Duygulu and S.R. Agnew, "Grain Size Effects on Deformation Mechanism Activity in Magnesium Alloy AZ31B", presented in the Magnesium Technology 2005 Symposium, TMS Annual Meeting, San Francisco, CA, Feb '05.

S.R. Agnew, D.W. Brown, and C.N. Tomé, "Neutron Diffraction Study of Deformation Mechanisms in Magnesium Alloy AZ31B," presented in the Symposium on Neutron Diffraction Characterization of Mechanical Behavior, ibid.

S.R. Agnew, A. Jain, and O. Duygulu, "Modeling the Temperature Dependent Effect of Twinning on Mechanical Behavior of Magnesium", 10th International Symposium on the Physics of Materials, Prague, Czech Republic, Aug '05.

D. Thermomechanical Processing of Ti and Ti-6Al-4V Sheet and Plate from Low Cost Powders

Principal Investigator: Craig A. Blue
Oak Ridge National Laboratory
Oak Ridge, TN 37831-8063
(865) 574-4351; fax (865) 574-4357; e-mail: blueca@ornl.gov

Field Project Manager: William H. Peter
Oak Ridge National Laboratory
Oak Ridge, TN 37831-8063
(865) 241-8113; fax (865) 574-4357; e-mail: rivardjd@ornl.gov

Chief Scientist: James J. Eberhardt
(202) 586-9837; fax: (202) 587-2476; e-mail: James.Eberhardt@ee.doe.gov
Field Technical Manager: Philip S. Sklad
(865) 574-5069; fax:(865) 576-4963; e-mail:skladps@ornl.gov

Participants:
Evan K. Ohriner, Oak Ridge National Laboratory
David C. Harper, Oak Ridge National Laboratory
Jim O. Kiggins, Oak Ridge National Laboratory
Paul A. Menchhofer, Oak Ridge National Laboratory
Lance Jacobsen, International Titanium Powder, L.L.C.
Dariusz Kogut, International Titanium Powder, L.L.C.

Contractor: Oak Ridge National Laboratory
Contract No.: DE-AC05-00OR22725

Objective

- Investigate and develop vacuum hot pressing (VHP) methods for the production of titanium (Ti) and Ti-6Al-4V plate from Ti and Ti-6Al-4V powder provided by International Titanium Powder, LLC (ITP).
- Demonstrate the ability to extrude rod using powder Ti precursor.
- Mechanically test Oak Ridge National Laboratory (ORNL) – consolidated materials.
- Optically and chemically analyze ORNL-produced materials.

Approach

- Conduct parametric studies using VHP to consolidate ITP Ti and Ti-6Al-4V powder to demonstrate the feasibility of powder use for automotive applications.
- Develop extrusion techniques for the production of Ti and Ti-6Al-4V from ITP powder.
- Characterize ORNL-produced material properties.
- Develop approach to scaling processing techniques for large-scale automotive production applications.

Accomplishments

- A preliminary parametric study of VHP was completed looking at the effect of temperature, stress, and time. Developed minimum limits of stress for the full consolidation of Ti plates.
- CP Ti plates as large as 270 mm in diameter and roughly 9 mm thick were pressed at temperatures between 550°C and 1500°C, and low pressure levels between 0.9 MPa and 5 MPa. These results were compared with previously reported VHP samples [1, 2].
- Ti and Ti-6Al-4V powders were successfully extruded.
- Evaluated physical, microstructural, and chemical properties of ORNL-produced materials.

Future Direction

- Partner with ITP and Ametek to scale process to produce Ti and Ti-6Al-4V sheet and plate at substantially reduced cost using pneumatic isostatic forging and extrusion processes as a basis for commercial processing.
- Partner with Universal Alloy Corporation to extrude ITP Ti and Ti-6Al-4V rod and plates up to 40 in. wide.

Introduction

The aircraft industry is currently the single largest market for Ti and Ti alloy products primarily because of the exceptional strength-to-weight ratio, elevated temperature performance, and corrosion resistance.

Titanium usage, however, is strongly limited outside the aerospace industry by its higher cost relative to competing materials, primarily aluminum alloys and steels. Although Ti possesses an attractive set of properties, including high specific strength and corrosion resistance, and allows for damage-tolerant design, cost limits applications to selected markets. Many automotive systems would benefit from the use of Ti products. Automotive exhaust systems could save as much as 50% of their current weight by integrating Ti parts. Titanium valves and valve springs, connecting rods, suspension springs, wheels, drive shafts, underbody panels, side impact bars, and half shafts are just some of the automotive applications that could benefit from the use of Ti.

The present market comparison for the use of engineering materials shows that steel is the most widely used material, with 800 million tons used each year. Aluminum, stainless steel, and copper are used at a rate of 22 million tons, 16 million tons, and 12 million tons, respectively. Titanium is much less widely used at 0.05 millions tons per year.

Potential technical problems preventing the integration of Ti, apart from cost of manufacturing, include wear resistance, a lower modulus than steel, and machining difficulties. Wear resistance can be addressed by coatings/reinforcements; the modulus can be increased by reinforcing the part with a second material; and the machining difficulties can be reduced by the production of near-net-shape parts. The major problem is that Ti costs substantially more than competing materials.

Although the cost of Ti ore is significantly more than that of other competing materials, the difference in the cost of sheet is a result of processing. Processing of Ti from ingot to plate accounts for 47% of the total cost of the material.

Current melting techniques include vacuum arc remelting (VAR), electron beam melting, and plasma arc single-melt processes. VAR is used to consolidate feedstocks, improve homogeneity and refine grain size. To VAR-cast an ingot, a dc arc is struck between a Ti electrode and a base plate. The intense heat melts the electrode, and the Ti is cast into an ingot. VAR requires 20 hours and large-scale equipment.

Electron beam and plasma arc single-melt processes have the advantage over VAR in increased use of low cost scrap and improved removal of high density and low density inclusions. In these two processes, ingots are cast directly from melted feed

sponge, alloy additions and scrap. But the cast ingot still requires post-processing, which accounts for 47% of the total cost.

Alternative processing methods such as casting, laser forming, and spray forming have also been explored. Casting is best suited for complex shape forming and is not economical for sheet processing. The process requires extensive tooling and frequent inspections. A post–hot isostatic pressing (HIP) is needed to eliminate porosity. Laser forming uses a raw powder stream injected into a rastered laser beam to melt, form, and build up sheet. Spray forming operates similarly, although a plasma torch melts the powder. Laser forming and spray forming have the advantages of using less material, requiring minimal tooling, and needing short cycle times. But it is difficult to control the thermal history of laser forming, and both methods suffer from residual porosity. In addition, both of these methods require conventionally produced and atomized powder, which is very costly.

Although much time and effort has been invested in the development of these processing techniques, the cost of Ti still remains high because of the cost of raw materials, cost of post-processing, and yield losses. Previous work performed at the Infrared Processing Center at ORNL, focused on the consolidation of low-cost Ti powder via preliminary VHP studies, high-density infrared (HDI) processing, and simulated roll compaction processing [1,2]. Recently, the Materials Processing Group at ORNL has investigated VHP of moderately sized parts at low pressures and extrusion of CP Ti and Ti alloys. Both processing methods used powder provided by ITP. ITP has developed a new low-cost method of powder production and is currently running a pilot processing facility.

Experimental Procedure

ITP Ti powder was processed into rod, flat stock, and plate using two methods, extrusion and VHP techniques. An off-stoichiometry alpha-beta ITP Ti alloy (used to establish processing parameters) and limited Ti-6Al-4V were processed into rods using extrusion techniques. Metallography, chemical analysis, and mechanical evaluation of the CP Ti extrusion followed. Metallography was performed on the Ti-6Al-4V extrusion sample, but limited powder prevented sufficient material for mechanical evaluation.

VHP, a batch process, was used to make Ti plates for the prototype production of Ti-brake rotors. VHP was used to make nine - 267 mm diameter Ti discs, 9 mm in thickness. Each sample was pressed under vacuum in a graphite element radiant furnace. For each of the pressing operations, the die was lined with Grafoil and around 1900 grams of Ti powder was poured into the die. Two independent production batches of low cost Ti from International Titanium Powder were used for the VHP evaluation. These runs were also separate from powder previously mentioned in the FY04 annual report [2]. To prevent mechanical interaction between air and the powder, no pre-pressing was applied until after a vacuum was pulled. A special collar was placed under the die to keep it in place while the powder was being pressed. When the rams were jogged into place, the furnace was closed, sealed, and evacuated. The furnace was back-filled with argon gas and evacuated three times in order to ensure a clean processing environment. The Ti samples were pressed at low pressures, between 0.8 and 4.9 MPa, and temperatures between 580 and 1500 ^{o}C. All samples were allowed to furnace cool after the heating cycle was completed. After the samples were removed from the furnace, the sample surfaces were sand blasted, and the densities were measured by immersion in ethanol (Archimedes method). Tensile specimens were machined out of several of the VHP discs. Mechanical testing, chemical analysis, and optical microscopy were performed. Mechanical testing was performed on plate specimens with a testing gauge section of ~1.47 mm in width and ~0.74 mm in thickness. The test gauge length was 20.32 mm. The monotonic tensile testing was performed with a strain rate of ~0.05 in/in·min based on constant cross head speed.

Four CP-Ti samples, one Ti-6Al-4V sample, and three off-stoichiometry alpha-beta Ti alloy samples were extruded. The powder for each extrusion was cold pressed in a 5.1 or 8.9 cm diameter steel can to a green density of approximately 20% of theoretical density. The cans were then electron-beam welded

in a vacuum chamber. All samples were extruded on ORNL material processing group's 1250 ton extrusion press. The Ti samples were preheated between 850°C and 950°C for 1.5 hours and then extruded up to a maximum load of 640 tons. The Ti-6Al-4V sample was preheated at 950°C for 2 hours and then extruded at a maximum load of 380 tons. The off-stoichiometry Ti alpha beta alloy cans were preheated at 925°C for 1.5 hours and then extruded up to a maximum load of 410 tons. Table 1 contains the preheat temperature and the die size for all Ti extrusions. Samples were de-canned. Tensile and metallography specimens were made from selected extruded samples. Figure 1 is an image of round and flat bar extrusion stock and tensile specimens made from the CP-Ti extrusions.

Results and Discussion

Successful production of low-cost Ti powder could be beneficial for promoting new, innovative applications that were not realized due to the high cost of Ti. Several of these applications could use the high strength to weight ratios. Brake rotors are one particular application that utilizes titanium for weight reduction. Particularly, vehicular racing, such as sprint car and midget car, utilizes Ti brake rotors to reduce the weight of conventional gray cast iron rotors. In this application, good ductility and corrosion resistance are not necessary. However, moderate plate diameters and strengths are necessary for the service conditions. Wear is a large concern for automotive brake rotors, but common practice is to coat the Ti rotor with a ceramic coating, such as alumina. Therefore, ORNL evaluated the consolidation of low-cost CP Ti powder into 267. mm Ti brake rotors for sprint car application.

A 64 mm and 178 mm fully consolidated plate had previously been produced with low-cost Ti, and was reported in last year's annual report [2]. Furthermore, the 64 mm plate exhibited mechanical properties and metallography comparable to grade 2 CP Ti specimens [1,2,3]. The purpose of this VHP parametric study was to obtain the lowest pressure and temperature required to consolidate large components with strengths comparable to CP grade 2 Ti.

The maximum pressure used in this parametric study, 4.8 MPa, was only approximately 10% of the pressure used to produce the 64 mm sample exhibiting textbook strengths and ductility.

The density of each plate was measured by the Archimedes method, and is listed in table 2, along with any mechanical results obtained and the processing parameters. All of the plates from the first Ti powder production batch were consolidated to 90% of the theoretical density of Ti with the exceptions of trials 1 and 2. Trial 1 was pressed at considerably low pressure, 0.9 MPa; trial 2 was pressed at low temperatures, 580°C. The processing pressure for satisfactory consolidation and strength seems to be a minimum of 1.8 MPa for this batch of

Table 1. Extrusion Parameters for Ti and Ti Alloy Low Cost Powder

Extrusion	Material	Preheat Temperature (°C)	Preheat Time (min.)	Can Diameter (cm)	Die Shape	Die Size (cm)	Extrusion Ratio	Max. Load (tons)
1-1	CP Ti	885	90	5.1	Round	2.0	6.3	380
2-1	CP Ti	950	90	8.9	Round	4.45	4.0	440
2-2	CP Ti	950	90	8.9	Round	3.25	7.5	490
2-3	CP Ti	850	90	8.9	Round	3.25	7.5	640
3-1	Ti-6Al-4V	950	120	5.1	Round	2.0	6.3	380
4-1	Off Stoich. α-β Ti	925	90	8.9	Round	3.25	7.5	410
4-2	Off Stoich. α-β Ti	925	90	8.9	Round	4.45	4.0	340
4-3	Off Stoich. α-β Ti	925	90	8.9	Rectangular	5.08x1.91	6.4	405

Figure 1. Extruded bars and flat stock after removing the can material and machined tensile specimens.

low-cost Ti powder. Low alpha phase temperatures, e.g., 580°C, are not sufficient for consolidation at low to moderate pressures. Temperatures ranging from near alpha transus temperatures (the alpha transus is around 890°C [3]) to beta phase temperatures seemed to be the best range for consolidation. However, temperatures in the range between 600°C and 850°C were not tested.

The chemistry of the low-cost Ti seems to play a role in the minimum pressure required for consolidation. A second batch of powder was consolidated; this powder would only consolidate to 86% of the theoretical density under similar VHP parameters as the first batch. The results can be seen as trials 8-9. Chemical analysis is being conducted on the two batches to understand the deviation, but a conclusion could not be made before submission of the annual report. Preliminary analysis of the two powders before consolidation did not show any outstanding quantities of oxygen, nitrogen, carbon, and/or iron compared to CP Ti grade 2 ASTM specifications. However, a broader evaluation is being conducted. Powder morphology may also play a significant role, and will be investigated.

The VHP plates showed excellent tensile strength, 545 MPa to 595 MPa. Elongation measured after failure was considerably low for Ti, between 1 to 5%. Once again, high ductility does not seem to be a necessary characteristic for brake rotor application; 1 to 5% is higher than most gray cast iron alloys. The Ti plates pressed from the second batch of powder had lower tensile strengths as would be expected for material consolidated only to 86% of the theoretical density; this material was still close to CP Ti grade 2 strength limitations.

Microstructural investigations were performed on the VHP Ti plates. Samples were cut from the as-pressed plates, mounted, polished, and etched with Kroll's reagent. Figure 2 is an optical micrograph of the VHP trial #3 sample using polarized light. This micrograph was representative of most of the samples where a standard equiaxed alpha Ti microstructure was present. However, porosity is visible throughout the cross section. An increase in the pressing load should eliminate this porosity, and increase the density to the theoretical density of Ti. The porosity could also be affecting the observed elongation.

Table 2. Consolidation results of 267 mm-diameter VHP Ti plates.

Description	Diameter (mm)	Pressure (MPa)	Temperature (°C)	Time (Hr)	Bulk Density (%)	Alcohol Density (%)	UTS (MPa)	Elongation (%)	Batch
Trial 1 – Low Pressure	267	0.9	865	1	71%	NM[1]	NM[1]	NM[1]	Batch 1
Trial 2 – Low Temperature	267	2.9	580	2.5	85%	NM[1]	NM[1]	NM[1]	Batch 1
Trials 3-7	267	1.7-4.5	885-1250	1-2	90-94%	92-94%	545-595	1-5	Batch 1
Trials 8-9 – Secondary Batch of Powder	267	2.8-4.8	900-1500	1	82-89%	87-88%	338	< 1	Batch 2
ORNL VHP Results of 64 mm Disc [1,2]	64	55.3	900	0.5	100%	100%	614	21	Previous Batch
ORNL VHP Results of 178 mm Disc [1,2]	178	11.7	900	1	100%	100%	614	21	Previous Batch
ASTM Grade 2 [3]	N/A	N/A	N/A	N/A	100%	100%	345	20	N/A

[1] NM = Not Measured.

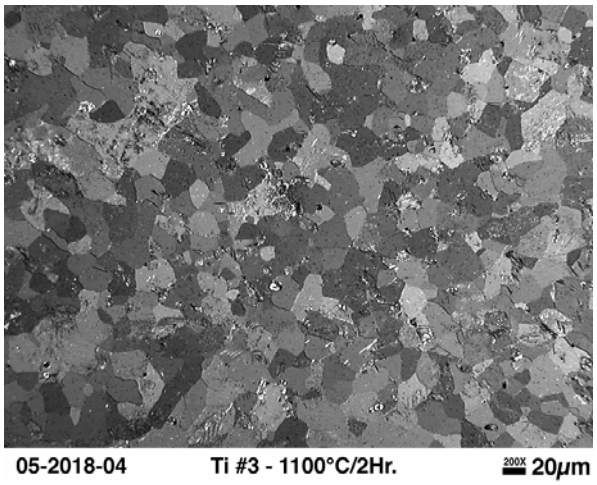

Figure 2. Microstructure for a Ti VHP sample #3.

After pressing, a few of the Ti plates were machined into sprint car brake rotors for demo components. Figure 3 shows an example of one of the plates machined into a disc rotor for sprint car application. The consolidated low-cost Ti powder did not cause any noticeable problems or changes to machining of the Ti components. Future VHP components may be pressed to near net shape, eliminating a great extent of the machining.

The cans with the Ti and Ti-6Al-4V powder were successfully extruded. Microstructural investigations were performed on the as-extruded Ti and Ti-6Al-4V bars. Samples were etched with Kroll's reagent. Figure 4 is an optical micrograph of one of the Ti extruded samples (left) and the Ti-6Al-4V sample (right). Table 2 contains the mechanical properties of the CP Ti sample extruded at 885°C. Other CP Ti samples are in the processes of being tested, but seem to have similar strength and ductility. The extruded low-cost Ti seems to have mechanical properties similar to Grade 2 CP Ti. The Ti-6Al-4V properties were inconclusive due to extremely small amounts of powder utilized and the machining of specimens from the can. Further investigation is being conducted. These results show a strong potential for the extrusion of ITP Ti powder.

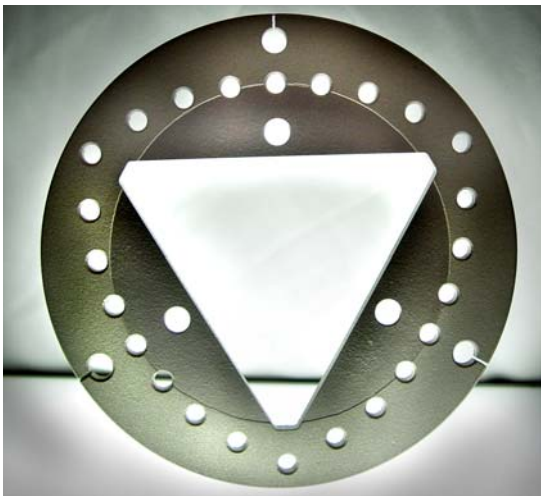

Figure 3. Machined Ti break rotor from 267 mm diameter VHP plate pressed at ORNL.

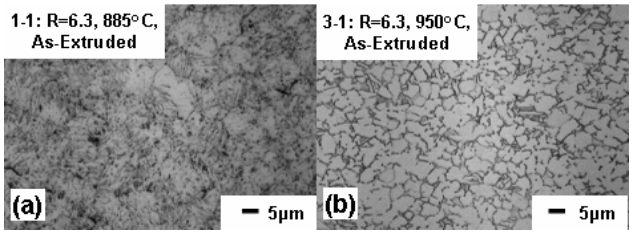

Figure 4. Microstructures for extruded (a) CP Ti and (b) Ti-6Al-4V, both had extrusion ratios, R, of 6.3.

Table 2. Mechanical testing results of as-extruded Ti samples.

Sample	Yield strength [MPa]	Tensile strength [MPa]	Elongation [%]
Extruded Ti 885°C R = 6.3	407	552	17.0
Ti Grade 2	345	448	20.0

Summary

These are the highlights of progress in FY 2005:

1. Production of VHP Ti plates up to 267 mm and the potential to be made into commercial parts.
2. Preliminary results indicate plates consolidated at low pressures can obtain tensile strengths within allowable limits. However, elongation is low compared to fully consolidate CP Ti.

3. Extrusion of Ti and Ti-6Al-4V rod was performed.
4. CP Ti extrusions had similar strength and ductility to Grade 2 CP Ti.

Conclusions

Although Ti and Ti-6Al-4V have attractive properties that would benefit a great number of engineering applications, their use is limited by the cost of the raw material and the processing that is necessary to make a usable product. But with the recent advancements in low-cost powder production at ITP, in conjunction with processing techniques developed at ORNL in collaboration with industry, the cost of Ti products could be drastically reduced. While VHP on a large scale may not be an economical method of plate production, it does demonstrate that ITP powder can produce a viable product, and make substantial parts. On the other hand, the extrusion processing of Ti powder could easily be adapted to industry with already existing equipment. The preliminary study of CP-Ti extrusions seems to produce mechanical properties similar to cast Ti. The ductility and strength of the Ti-6Al-4V was inconclusive due to minimal powder utilized; full investigation of Ti-6Al-4V with sufficient material may result in production of materials with commercial properties. Results suggest that the extrusion and pneumatic isostatic forging of low cost Ti based materials for automotive applications are highly feasible and will be further explored.

References

1. J.D.K. Rivard, C.A. Blue, D.C. Harper, J.O. Kiggans, P.A. Menchhofer, J.R. Mayotte, L. Jacobsen, and D. Kogut. "The Thermomechanical Processing of Titanium and Ti-6Al-4V Thin Gage Sheet and Plate," *JOM*, 57(11), 2005.
2. FY 2004 Progress Report for High Strength Weight Reduction Materials.
3. R. Boyer, G. Welsch, and E.W. Colligs (Eds). Materials Properties Handbook: Titanium Alloys. ASM International. pgs. 165-260, 1994.

E. Counter Gravity (Hitchiner) and Pressure Assisted Lost Foam Magnesium Casting

Principal Investigator: Qingyou Han
Oak Ridge National Laboratory
Oak Ridge, TN 37831-6083
(865) 574-4352; fax (865) 574-4357; e-mail:hanq@ornl.gov

Chief Scientist: James J. Eberhardt
(202) 586-9837; fax: (202) 587-2476; e-mail: James.Eberhardt@ee.doe.gov
Field Technical Manager: Philip S. Sklad
(865) 574-5069; fax: (865) 576-4963; e-mail:skladps@ornl.gov

Participants:
Ralph B. Dinwiddie, Oak Ridge National Laboratory
Pete Angelini, Oak Ridge National Laboratory
Graham V. Walford, Walford Technologies
Ken Currie, Tennessee Technological University
Mohamed Abdelrahman, Tennessee Technological University
Fred Vondra, Tennessee Technological University

Contractor: Oak Ridge National Laboratory
Contract No.: DE-AC05-00OR22725

Objective

The objective of this project is to evaluate the Hitchiner process and pressure assisted lost foam casting of magnesium alloys, in particular, the project will

- Develop the casting system
- Develop low density foams and appropriate coatings
- Establish casting parameters for selected magnesium alloys
- Conduct computer simulations of the process to be used to generate design guidelines
- Validate the process by characterizing microstructure and properties of castings

Approach

- Compare lost foam casting characteristics of magnesium and aluminum at 1 atmosphere
  - Plate casting
    - Flow, mold filling, metal/mold/coating interactions
    - Integrity: porosity, oxide content, microstructure, and mechanical properties
  - Complex casting
    - Castability/integrity/mechanical properties
- Compare lost foam Mg casting with Hitchiner lost foam Mg casting (pressure assistant)
  - Castability/integrity/mechanical properties

- Document the features of the Hitchiner lost foam Mg casting
  - Possible applications, typical features of casting that are suitable for the Hitchiner process, and limitations of the Hitchiner process

Accomplishments

- Melting and casting capabilities have been developed at Tennessee Technological University and Oak Ridge National Laboratory
- Simulation tools have been prepared for the prediction of lost foam castings
- A system has been developed for the selection of foam materials and coatings
- Experiments have been carried out to develop baseline data and to evaluate the lost foam process

Future Direction

- Select/develop coatings and foams for lost foam magnesium casting
- Complete the design of parametric study of the parameters affecting the castability of magnesium alloys
- Start the simulation of the Hitchiner/lost foam process
- Analyze mold filling and molten metal/foam interactions.

Introduction

The last 10 years have seen a dramatic increase in the production and utilization of magnesium. This demand is primarily due to an increase of 20% annually in the use of magnesium in the automobile industry driven by the desire to increase vehicle fuel efficiency by reducing vehicle weight. Magnesium has found uses in several automotive components because of its low density and high strength-to-weight ratio as compared to conventional automotive materials. More recently, magnesium castings have been introduced into pick-up trucks and vans such as the standard size Ford F-150. Additional opportunities exist for the use of magnesium casting in these vehicles, as well as, in heavier trucks. Even with these successes, however, magnesium has not been so widely accepted as it might have been for the following reasons: the cost of the alloys, the lack of long-term field validation or controlled fleet testing data for powertrain components, and lack of a technological base for foundry casting of magnesium alloys.

Magnesium castings are traditionally produced by die casting or precision sand casting. Each of these processes has its advantages and disadvantages for producing components. The major disadvantage of the conventional processes is that certain geometries cannot be produced using steel die sections and are limited by moving cores. In addition, die casting often results in unacceptable levels of porosity. On the other hand, precision sand casting can produce a wide range of shapes with high levels of soundness, but at an unacceptable cost. While successful castings can be manufactured, continuing problems experienced during the casting of the magnesium alloys include porosity formation, oxidation, and hot tearing/crack formation.

In order to take greater advantage of the attractive properties of magnesium, alternative approaches that promise to be more robust and lead to the development and fabrication of larger thinner wall castings must be considered. Lost foam castings can be competitive with other casting techniques for applications with complex internal passages (coring) that can reduce machining, save space, and/or integrate multiple complex features or components into a single casting.

Previous studies at Oak Ridge National Laboratory on gravity lost foam casting of aluminum have determined that many factors affect the quality of the casting outcome. In particular, the metals filling process of the lost foam pattern is greatly influenced by the pattern properties. The advancing metal front decomposes the foam into gaseous and liquid decomposition products that must be eliminated from the casting volume to complete the process.

Pattern density and the pattern gas permeability arising from the combination of the foam and ceramic coating are critical factors in the process, yet are not measured on any commercial process line. Variances in these properties are difficult to control and result in variance in the metal filling behavior. The physical properties of magnesium would increase this problem further. In particular, the low density and latent heat, and the high reactivity of the molten magnesium alloy are serious issues for its castability under lost foam casting conditions.

The problems described above can be overcome by making use of pressure/vacuum assisted mold filling together with closed loop process control. The Hitchiner process, which uses vacuum as a driving force for mold filling, is a logical choice for lost foam casting of magnesium alloys. The change of pressure across the advancing metal front can then be used to accommodate variances in the gas permeability of the foam and coating for the whole pattern and for local variations in the pattern. Pressure can also be used to assist in mold filling.

The challenges of using the Hitchiner process and pressure assisted lost foam Mg casting are in the areas of setting up the experimental equipment for the research, a parametric study of the parameters affecting the processes, development of low density foams for the casting of magnesium alloys, control of permeability of the sand, foam and foam coatings, and the use of controlled atmospheres for reducing metals reactance chemistry and the thermal profile of the pattern to be cast. This article is the first year report of the project. The goal of the first year research was to develop the casting system and to evaluate the existing lost foam casting process for magnesium and aluminum alloys.

The Casting Systems

The existing metalcasting facilities at TTU have been modified for handling molten magnesium alloys and for counter gravity lost foam casting of magnesium alloys. A Thermtronix Solid State Aluminum/Magnesium Electric Resistance Furnace has been purchased and is currently being facilitated for use. It has a 200-300 pound charge capability (depending on whether it is used for magnesium or aluminum) and a special purpose cover made from mild steel has been added to the furnace to allow for introduction of a cover gas to prevent the molten magnesium alloys from reacting with the atmosphere. The cover also has a hinged lid on the very top to facilitate direct insertion of the counter gravity sprue. The Hitchiner counter gravity casting system, shown in Figure 1, has also been successfully tested for aluminum castings. Both a simple flat plate pattern (GM provided) and widget pattern (Foseco Morval provided) were successfully cast using aluminum alloy 319. A 1% Sulfur Hexafluoride – 99% Carbon Dioxide cover gas will be used over the molten magnesium either in the crucible or the furnace. A set of safe operating procedures have been adopted to safely handle and cast magnesium alloys in the current casting facility. However, to better facilitate a safer work environment, an additional 1,200 sq. ft. of foundry space is in the process of being specified and built directly behind the current TTU Foundry facility. An additional $20,000 has been committed from the local AFS Tennessee chapter and the Foundrymen's Education Foundation for supplementing the construction costs. Expected completion of the facility is expected within the next several months. Until the new facility comes on-line, additional safety procedures within the existing foundry are being undertaken to ensure that project deliverables can be met.

Figure 1. The Hitchiner casting system located at TTU.

Foam Development and Selection

A broader study of foam decomposition has been undertaken that seeks to develop a kinetic and thermo-chemical model that describes polystyrene foam decomposition for a broad range of heating rates for oxidizing and non-oxidizing environments. Understanding the foam decomposition processes under different process conditions including foam decomposition in the presence of molten magnesium served as the motivation behind this work. This might help in improving casting quality such as reducing residue entrainment.

A thorough literature search was conducted to find an appropriate kinetic model applicable to the polystyrene foam decomposition phenomena encountered in the lost foam casting process. Results of this investigation indicate that the process conditions in which the available models were developed were very different from the casting process conditions, and hence no one model could be suitably employed for the LFC process. A more rigorous and intrinsic kinetic experiment, depicting the actual foundry conditions, is necessary to develop a model that describes the foam degradation kinetics.

The main purpose of this experimentation is to obtain data on the composition of polystyrene foam degradation products as a function of melt temperatures and processing times. The challenge lies in developing a technique and apparatus for a small-scale kinetic study, which simulates the LFC process conditions and also which eliminates or minimizes the gas phase transients experienced on the commercial scale.

Initially a simple burn chamber using an Infra-red heat source was constructed for these experiments but a more precise reactor concept was conceived. Figure 2 shows the burn chamber to be used. The reactor consists of a heater maintained at a constant surface temperature, an automatic feeder that feeds the foam at a velocity 'v' from the automatic feeder, which simulates the actual metal temperature and melt flow rate respectively in the commercial casting process. When the foam impinges on the heater surface, it decomposes and forms various products. These liquid and gaseous products are

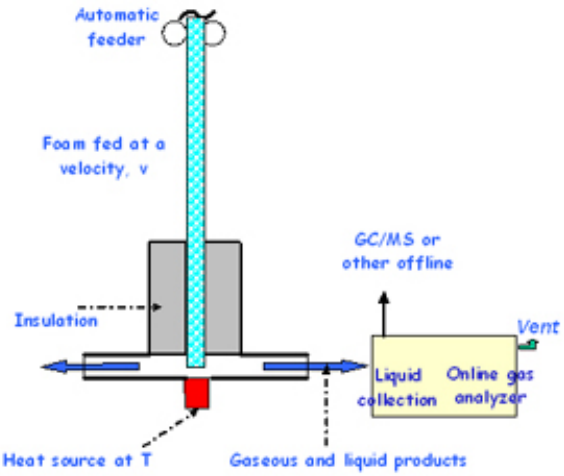

Figure2. The burn chamber for characterizing foam decomposition.

collected and analyzed for their composition. Decomposition data could be collected as a function of both foam push rate and metal temperature. A schematic of the proposed reactor is shown in the figure.

The Reactor heater design considerations include a uniform surface temperature profile on the heater surface, which is very important to carry out this kinetic study. Also, the surface has to be maintained at a steady temperature throughout the process. A "huge" melt (metal anvil) is needed to withstand the high heat of degradation. The heating anvil was modeled in FEMLAB to determine the total power required for the process. A simple anvil geometry was constructed and byusing FEMLAB's built-in heat transfer modules, a detailed parametric study was performed and the anvil sizing determined. Design of the exit ports of the reactor is currently in progress. Careful attention is paid to reduce the backpressure/pressure inside the reactor by suitably sizing the exit ports. Provisions for the gas inlet are also being considered so that the kinetic study could be performed under different oxidizing and non-oxidizing environments. The effect of materials used for the construction of the heating anvil and insulations are also being studied so as to improve the heater efficiency by reducing heat losses.

In addition to analyzing and modeling the foam decomposition products, another important aspect of this line of research is the gas diffusion modeling and experiments. In order to study the behavior of

polystyrene foam under the extreme conditions of very high temperature and high heating rates, it is important to understand the gas diffusion phenomena through the polystyrene foam itself and also when a coating is applied. This would be helpful to suitably manufacture foam so that the gas diffusion could be better controlled. Once this is achieved, the foam decomposition could be controlled by carrying out the process in suitable environments. Although there are some diffusion models available in the literature, they generally do not take into account the heterogeneity present in the foam. A number of factors account for this heterogeneity, including broken cell walls, open channels, fusion level,etc. Hence a multi-scale approach was developed to measure the gas diffusion coefficients through the cell wall (mimicked with a polystyrene film) in order to develop the model for gas diffusion through the foam. By studying the morphology, a suitable entity would be included in the model to account for the heterogeneity in the foam.

Mold Filling and Metal/Foam Interactions

Experiments have been carried out at ORNL for observing mold filling and metal/foam interactions during both aluminum lost foam casting and magnesium lost foam casting at gravity casting conditions (one atmosphere). The purpose was to establish baseline data of lost foam casting at one atmosphere. The data will be used for comparing with data obtained in the Hitchiner process and the pressure assisted lost foam casting process.

Two types of patterns were used: one was a simple flat plate and the other was the GM window pattern. The plate pattern was used for observing mold filling and for evaluating porosity distribution. The window pattern was used for evaluating the castability of alloys. Five types of foam materials from Styrochem were tested: type A (T-17-170, ventless tool), type B1 (T-185, vented tool), type B2 (T-185, ventless tool), type C (T-170, vented tool), and type E (T-185 with Bromated additive, ventless tool). A high permeability coating was used for the testing. Castings of A356 alloy and AM60B alloy were made using the flat plate pattern and the GM window pattern.

Figure 3 shows the effect of casting temperature on the castability AM60B alloy. Castings were made using the GM window patterns made of B1 foam. The pouring temperature or the cast temperature has a major effect on the castability of the AM60B alloy window casting. Cold shot defect occurred at the corner where the metal filled last when the pouring temperatures were around 1400°F to 1450°F. Increasing the pouring temperature reduces the cold shot defect. When the pouring temperature was 1500°F, the cold shot defect was eliminated. However, 1500°F is about 355°F higher than the liquidus temperature of the alloy. Similar window castings were also made using A356 alloy, which has the identical liquidus temperature as the AM60B alloy. All the A356 alloy window castings had no cold shot defect when the pouring temperature was as low as 1400°F. Thus it is more difficult to cast magnesium alloy castings using the lost foam casting process.

An infra-red camera was then used to observe mold filling and metal/foam interactions of AM60B and A356 alloy during lost foam casting. The use of the infra-red camera made it possible to accurately measure the filling time. Figure 4 shows the measured filling times for the flat plate casting and the GM window casting. It took much longer time to fill the lost foam mold for magnesium alloy than that for aluminum alloy. Indeed, the density and the latent heat of magnesium alloy are smaller than that

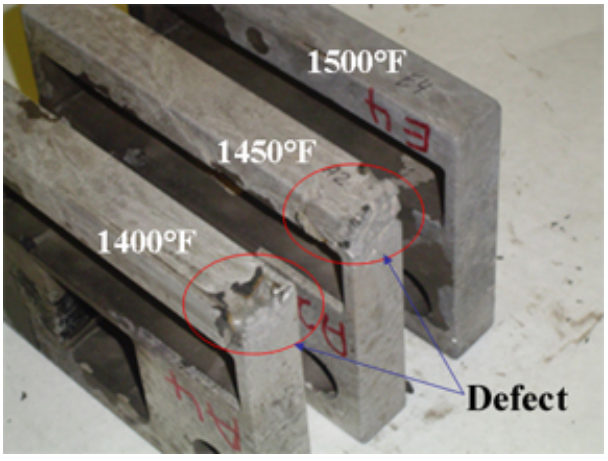

Figure 3. The cold shot defect at the corner of a GM window casting. The corner was the region last filled during mold filling. The defect can be reduced and finally eliminated by increasing the pouring temperature.

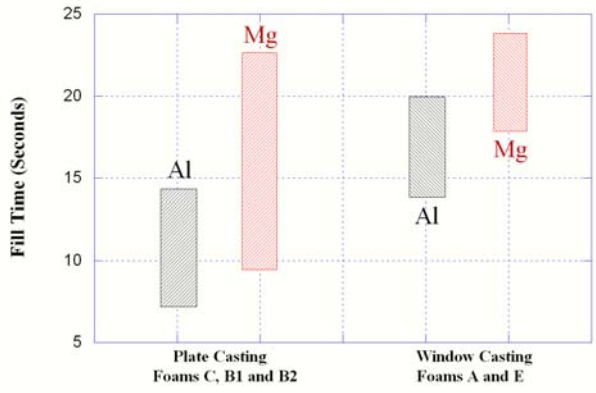

Figure 4. The measured fill time during lost foam casting of AM60B alloy and A356 alloy. The fill time is much longer for magnesium alloy than that for aluminum alloy.

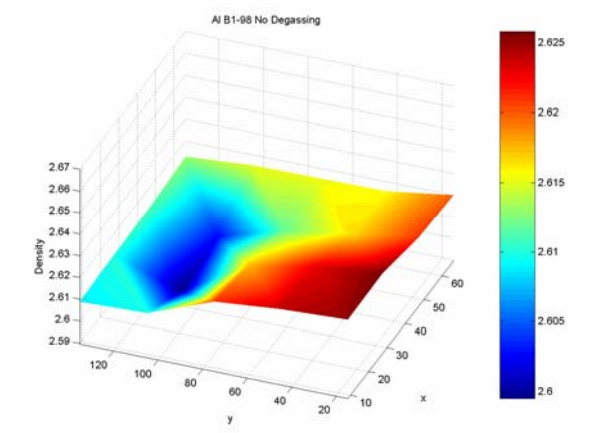

Figure 5. The measured density distribution in a lost foam aluminum A356 casting (flat plate casting not degassed). The casting was gated at the right side. A low density region is identified near the left side of the casting.

of the aluminum alloy. As a result, less heat is available for the molten magnesium alloy to decompose the foam when compared with aluminum alloy. This accounts for the fact that cold shot defect occurs more easily during lost foam magnesium casting than during lost foam aluminum casting.

The microstructure of the castings were also characterized, especially porosity distributions. Flat plate castings were cut into small specimens. Each specimen was used for density measurement using the apparent density measurement method. Figure 5 shows the density distribution in a flat plate casting of aluminum alloy not degassed. The gate location is at the right side of the plate (x=35 and y=20). The local density is high near the gate and low away from the gate. A low density region occurs near the end of the plate. A significant amount of porosity exists in this region. Figure 6 shows the pattern of mold filling obtained using the infra-red camera. The metal advances faster near the edge of the plate casting because of the decompose product of the foam can easily escape from the edges. As a result, the flow front is V shaped. The low porosity region occurs at the center of the V shaped region partly because of entrapped foam residues and partly because of the fact that the metal front collects more hydrogen as it is in contact with decomposed atmosphere for a longer time than the metal away from the front.

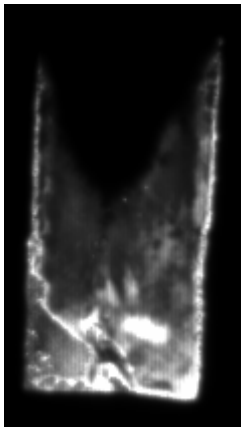

Figure 6. An Infra-red image of the flow front of the molten aluminum A356 alloy during mold filling. The flow advances faster near the edges of the casting, forming a V-shaped flow front. Foam residuals tend to be entrapped by this V-shaped front at the end of mold filling.

The flat plate casting made using degassed aluminum contained less porosity and hence had higher density than the undegassed aluminum. Figure 7 shows the density distribution of the degassed aluminum plate casting. The density of the casting is higher than 2.634. However, a low density region still exists near the end of the flat plate casting. The comparison of the degassed and undegassed lost foam casting suggests that the hydrogen content in the bulk melt contributes to the

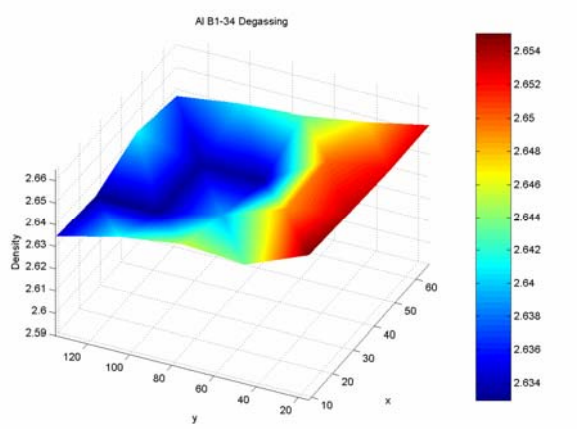

Figure 7. The measured density distribution in a lost foam aluminum casting when the molten metal was degassed before pouring. The density distribution is identical to that without degassing but density values are much higher in the degassed casting than in the undegassed casting.

porosity formation as well as the metal/foam reactions during lost foam casting of aluminum alloys.

The density distribution of the magnesium flat plate casting is shown in Figure 8. The density distribution is almost uniform throughout the casting. Unlike lost foam aluminum castings, the density distribution in lost foam magnesium casting is insensitive to the hydrogen content in the bulk melt. Degassing is not significantly affecting the porosity distribution in the magnesium lost foam casting.

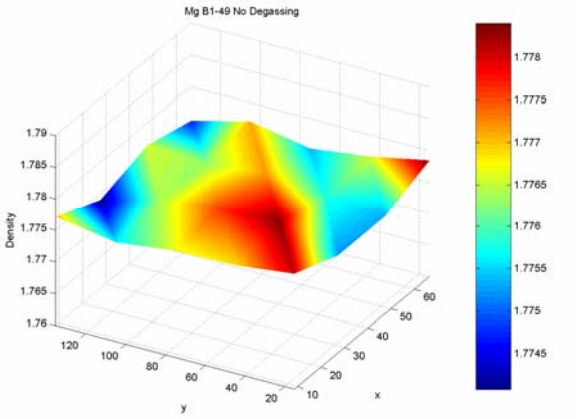

Figure 8. The measured distribution in a lost foam magnesium casting. The density values are fairly uniformly distributed throughout the casting.

Conclusions

The objectives of the first year research of this project have been completed. Melting and lost foam casting capabilities have been developed at the Tennessee Technological University and at Oak Ridge National Laboratory. These capabilities can be used for testing counter gravity (Hitchiner) and pressure assisted lost foam magnesium casting. A burn chamber has been developed/modified for studying polystyrene foam decomposition for a broad range of heating rates for oxidizing and non-oxidizing environments. This burn chamber will be used to quantify liquid pyrolysis behavior for its chemical and physical properties in normal and differing atmospheres. Lost foam castings of magnesium and aluminum alloys have been made.

Presentations/Publications/Patents

Q. Han and H. Xu, "Fluidity of Alloys under High Pressure Die Casting Conditions," Scripta Materialia., 2005, vol. 53, pp. 7-10.